ARTHRITIS & RHEUMATOLOGY
Vol. 0, No. 0, Month 2018, pp 1–13
DOI 10.1002/art.40467

Role of *Lgals9* Deficiency in Attenuating Nephritis and Arthritis in BALB/c Mice in a Pristane-Induced Lupus Model

Sonia Zeggar,[1] Katsue S. Watanabe,[1] Sanae Teshigawara,[1] Sumie Hiramatsu,[1] Takayuki Katsuyama,[1] Eri Katsuyama,[1] Haruki Watanabe,[1] Yoshinori Matsumoto,[1] Tomoko Kawabata,[1] Ken-ei Sada,[1] Toshiro Niki,[2] Mitsuomi Hirashima,[2] and Jun Wada[1]

Objective. **In systemic lupus erythematosus (SLE), an autoimmune disease associated with multiple organ involvement, the development of lupus nephritis determines prognosis, and arthritis impairs quality of life. Galectin 9 (Gal-9, *Lgals9*) is a β-galactoside–binding lectin that has been used for clinical application in autoimmune diseases, since recombinant Gal-9, as a ligand for T cell immunoglobulin and mucin domain–containing protein 3 (TIM-3), induces apoptosis of activated CD4+TIM-3+ Th1 cells. This study was undertaken to investigate whether deficiency of *Lgals9* has beneficial or deleterious effects on lupus in a murine model.**

Methods. **Gal-$9^{+/+}$ and Gal-$9^{-/-}$ female BALB/c mice were injected with pristane, and the severity of arthritis, proteinuria, and levels of autoantibody production were assessed at several time points immediately following injection. At 7 months after pristane injection, renal pathologic features, the severity of joint inflammation, and formation of lipogranulomas were evaluated. Subsets of inflammatory cells in the spleen and peritoneal lavage were characterized, and expression levels of cytokines from peritoneal macrophages were analyzed.**

Results. ***Lgals9*** **deficiency protected against the development of immune complex glomerulonephritis, arthritis, and peritoneal lipogranuloma formation in BALB/c mice in this murine model of pristane-induced lupus. The populations of T cell subsets and B cells in the spleen and peritoneum were not altered by *Lgals9* deficiency in pristane-injected BALB/c mice. Furthermore, *Lgals9* deficiency protected against pristane-induced lupus without altering the Toll-like receptor 7–type I interferon pathway.**

Conclusion. **Gal-9 is required for the induction and development of lupus nephritis and arthritis in this murine model of SLE. The results of the current investigation provide a potential new strategy in which antagonism of Gal-9 may be beneficial for the treatment of nephritis and arthritis in patients with SLE through targeting of activated macrophages.**

Systemic lupus erythematosus (SLE) is a multiorgan autoimmune disease that is characterized by a wide array of clinical manifestations and multifactorial pathogenic pathways. The disease process of SLE involves genetic, epigenetic, hormonal, and environmental factors, all of which ultimately lead to a disturbance in the pathways of both innate and adaptive immunity. Despite notable progress in the understanding of this disease, its etiology remains unclear and is still to be unraveled. Kidney involvement in SLE is known to be associated with poor clinical outcomes, with 10–30% of young patients developing end-stage renal disease (ESRD) (1,2). Despite the wide availability of different regimens involving treatment with immunosuppressant agents, many of which have undoubtedly improved the prognosis and survival of patients with SLE, an increased risk of ESRD in SLE has been observed since the late 2000s (3).

In contrast to lupus nephritis, lupus arthritis is one of the frequently encountered manifestations in

Supported by the Japan Society for the Promotion of Science (Grant-in-Aid for Scientific Research grants 26293218, 17K09976, 16K19600, and 16K09896).

[1]Sonia Zeggar, MD, Katsue S. Watanabe, MD, PhD, Sanae Teshigawara, MD, PhD, Sumie Hiramatsu, MD, Takayuki Katsuyama, MD, PhD, Eri Katsuyama, MD, PhD, Haruki Watanabe, MD, Yoshinori Matsumoto, MD, Tomoko Kawabata, MD, PhD, Ken-ei Sada, MD, PhD, Jun Wada, MD, PhD: Okayama University Graduate School of Medicine, Dentistry and Pharmaceutical Sciences, Okayama, Japan; [2]Toshiro Niki, MD, PhD, Mitsuomi Hirashima, MD, PhD: Kagawa University, Takamatsu, Japan.

Dr. Wada has received speaking fees and/or honoraria from Astellas, Boehringer Ingelheim, Novartis, and Tanabe Mitsubishi (less than $10,000 each) and grant support from Astellas, Bayer, Chugai, Daiichi Sankyo, Kissei, Kyowa Hakko Kirin, MSD, Otsuka, Teijin, Torii, Pfizer, Takeda, and Taisho Toyama.

Address correspondence to Jun Wada, MD, PhD, Department of Nephrology, Rheumatology, Endocrinology and Metabolism, Okayama University Graduate School of Medicine, Dentistry and Pharmaceutical Sciences, 2-5-1 Shikata-cho, Kita-ku, Okayama 700-8558, Japan. E-mail: junwada@okayama-u.ac.jp.

Submitted for publication August 1, 2017; accepted in revised form February 20, 2018.

SLE patients, and yet it may be overlooked behind the life-threatening conditions of lupus nephritis and neuropsychiatric SLE. Although few SLE patients develop full joint deformations, known as rhupus hands (4), lupus arthritis is a major cause of pain and discomfort and can impair the quality of life of patients (5).

Galectin 9 (Gal-9), a ubiquitously expressed β-galactoside–binding lectin (6,7), belongs to the tandem repeat subclass of the galectin superfamily, and is characterized by the presence of 2 distinct carbohydrate recognition domains joined by a link peptide (8). Among the 15 members of the galectin family, Gal-9 has been shown to function in both physiologic and pathologic conditions such as organogenesis, immune reactions, carcinogenesis, and metastasis (9). Gal-9 demonstrates bivalency and is able to cross link 2 glycoconjugates, and thus it is involved in the process of cell-to-cell and cell-to-matrix interactions. Results of recent investigations have suggested that the most dominant Gal-9 isoform, Gal-9Δ5, prevents metastasis by maintaining tissue integrity and inhibiting tumor migration and extravasation, while other Gal-9 isoforms facilitate metastasis (10). Gal-9 also modulates the processes of cell survival, such as apoptosis and cell cycle control, and induces apoptosis of various cell lines, such as the human melanoma cell line, T cell lines, and different types of leukemia cell lines (11,12).

In addition to the role of Gal-9 in cancer biology, it is involved actively at various stages of the immune response, and most of its effects are concentration dependent (13). Exogenous Gal-9 induces maturation of dendritic cells (DCs) associated with the up-regulation of costimulatory molecules such as CD40, CD54, CD80, CD83, and HLA–DR (14). The recombinant N-terminal Gal-9 is also effective in activating DCs by inducing a higher production of tumor necrosis factor (TNF) and interleukin-6 (IL-6), and greater phosphorylation of p38 and Akt (15). Through its divalent sugar-binding activity, Gal-9 forms Gal-9–glycan lattices with cell surface glycoproteins, which play major roles in the organization of cell membrane domains, regulation of thresholds of cell signaling, and receptor residency time on the cell surface (16). The local concentrations of Gal-9 and glycoconjugates determine the patterns of lattice formation and cellular response. At higher concentrations, Gal-9 induces apoptosis of CD4+ and CD8+ cells, while at lower concentrations, it increases cytokine production in activated T cells. T cell immunoglobulin and mucin domain–containing protein 3 (TIM-3), a glycoprotein with an *N*-glycan chain, is expressed on activated Th1 and Th17 cells. Gal-9 triggers calcium mobilization and activation of caspase 1, drives the apoptosis of Th1 and Th17 cells, and eliminates activated and exhausted T cells (11,17). In addition to Th1 cells, Gal-9 also induces apoptosis of B cells (B-lineage acute lymphoblastic leukemia 1 cells), monocytes (THP-1 cells), and myelocytes (HL-60 cells) (11). However, Gal-9 has not been found to exert apoptotic potential against Th2 and Treg cells lacking cell surface expression of TIM-3 (18,19).

The apoptotic potential of recombinant Gal-9 against immune-mediated cells prompted researchers to investigate the efficacy of recombinant Gal-9 in various disease models, such as experimental animal models of collagen-induced arthritis (CIA) (17,20,21), asthma (22), anti–glomerular basement membrane disease (23), lupus nephritis (24), diabetic nephropathy (25), and autoimmune encephalitis (17,26). In general, the apoptotic potential of Gal-9 is concentration dependent. A higher dose of recombinant Gal-9 induces apoptosis of Th1 and Th17 cells; however, a decline in its concentration by degradation may, inversely, stimulate CD4+ T cells, CD8+ T cells, and DCs to produce cytokines and chemokines.

Taking these findings into consideration, we investigated whether a total loss of Gal-9 would ameliorate or aggravate disease activity in a murine model of lupus, and determined whether blockade of Gal-9 and its signals might be beneficial in the treatment of SLE. To achieve this, we examined the effect of gene deletion of *Lgals9* (a gene encoding Gal-9) in BALB/c mice with pristane-induced lupus (27). This lupus model is associated with intraperitoneal lipogranulomas, diffuse proliferative glomerulonephritis (28), production of autoantibodies (29), and an erosive arthritis resembling rheumatoid arthritis (30). We also investigated the effect of *Lgals9* gene deficiency in a model of spontaneously induced SLE, using MRL/MpJ-Fas^{lpr}/J mice with a mutation in the gene encoding *Fas*. This model is associated with a defect in lymphocyte apoptosis and the impaired clearance of lymphocytes (31), high titers of autoantibodies, hypergammaglobulinemia, nephritis, vasculitis, and lymphadenopathy (32).

MATERIALS AND METHODS

Pristane-induced lupus model in BALB/c mice. BALB/c mice deficient in Gal-9 (Gal-9$^{-/-}$) were kindly provided by GalPharma (33,34). Using standard breeding techniques, Gal-9$^{-/-}$ BALB/c mice were crossed with BALB/cJ mice (The Jackson Laboratory) for 2 generations, and Gal-9$^{+/-}$ BALB/cJ mice were also bred, to obtain Gal-9$^{+/+}$ and Gal-9$^{-/-}$ littermates. Gal-9$^{-/-}$ female BALB/c mice (n = 12) and age- and sex-matched control Gal-9$^{+/+}$ mice (n = 12) were housed under specific pathogen–free conditions in a 12-hour light/dark cycle, with free access to water and standard rodent chow. The mice were injected intraperitoneally with 0.5 ml of pristane (chemical name 2,6,10,14-tetramethylpentadecane; Sigma-Aldrich) at age 7 weeks. Pristane-injected Gal-9$^{+/+}$ and Gal-9$^{-/-}$ BALB/c mice were designated as Gal-9$^{+/+}$ PI

and Gal-9$^{-/-}$ PI mice, respectively. During the course of the experiments, 1 of the Gal-9$^{+/+}$ PI mice accidentally died 4 months after pristane injection.

The severity of arthritis in the paws was evaluated every 2 weeks, and serum and urine samples were collected monthly. Peritoneal lavage, lipogranulomas in the peritoneal cavity, and spleen, kidney, and paw tissue were obtained at 7 months after pristane injection. For the characterization of Ly-6C^{high} monocytes and isolation of peritoneal macrophages, mice were euthanized at various time points: Gal-9$^{+/+}$ PI mice (n = 5) and Gal-9$^{-/-}$ PI mice (n = 5) at 24 hours after pristane injection, Gal-9$^{+/+}$ PI mice (n = 4) and Gal-9$^{-/-}$ PI mice (n = 4) at 15 days after pristane injection, and Gal-9$^{+/+}$ PI mice (n = 3) and Gal-9$^{-/-}$ PI mice (n = 3) at 4 weeks after pristane injection. For analysis of *Tnf* messenger RNA (mRNA) expression and quantification of TNF proteins, groups of Gal-9$^{+/+}$ PI mice (n = 4 per group) and Gal-9$^{-/-}$ PI mice (n = 4 per group) were euthanized at 4 hours, 24 hours, and 48 hours after pristane injection.

Generation of Gal-9$^{-/-}$ MRL/MpJ-Fas^{lpr}/J (MRL/lpr) mice. We generated Gal-9$^{-/-}$ MRL/lpr mice by mating Gal-9$^{-/-}$ female BALB/c mice with male MRL/lpr mice, to yield heterozygous F1 offspring. Gal-9$^{+/-}$ female F1 mice were further backcrossed with male MRL/lpr mice for 8 generations. Finally, Gal-9$^{+/-}$ F9 mice were intercrossed to obtain Gal-9$^{-/-}$ female MRL/lpr littermates (n = 15) and Gal-9$^{+/+}$ MRL/lpr littermates (n = 15). These mice were further monitored until age 16 weeks. Serum was collected at 8 and 16 weeks of age, while weight and proteinuria were assessed from 6 weeks of age and every 2 weeks thereafter. Tissue samples, including those from the spleen, lymph nodes, and kidneys, were obtained at the study end point.

All of the experimental procedures were approved by the Animal Care and Use Committee of the Department of Animal Resources, Advanced Science Research Center at Okayama University.

Determination of arthritis severity score. The mice were examined for the onset and severity of arthritis every 2 weeks after pristane injection. For scoring of arthritis severity, we used a previously published scoring system (35,36) with modification, as follows: score scale of 0–3, where 0 = normal, 1 = slight swelling or erythema of the wrist/ankle joint or footpad, 2 = moderate swelling and erythema of the wrist/ankle joint or footpad, and 3 = severe swelling and erythema of the paw. The scores for individual limbs were summed to obtain a total clinical arthritis severity score of 12 per animal. The incidence of arthritis was determined as the percentage of mice that had developed redness or swelling in at least 1 paw (representative images are shown in Supplementary Figure 1, available on the *Arthritis & Rheumatology* web site at http://onlinelibrary.wiley.com/doi/10.1002/art.40467/abstract).

Evaluation of histologic features and scoring of tissue samples. Samples of mouse kidney tissue were fixed in 10% formalin, and 4-μm paraffin-embedded sections were stained with hematoxylin and eosin (H&E), periodic acid–Schiff, periodic acid–methenamine silver, and Masson's trichrome stain. After H&E staining, glomerular hypercellularity was evaluated by counting the number of nuclei per glomerular cross-section (20 glomerular cross-sections per mouse), and tubulointerstitial nephritis was scored as previously described (37). For immunofluorescence analysis, the tissue samples were embedded in OCT compound (Sakura, Japan), and 4-μm cryostat sections were stained with fluorescein isothiocyanate (FITC)–conjugated goat anti-mouse IgG or rabbit anti-mouse C3 (Cappel). For analysis of IgG subclasses, the sections were stained using FITC-conjugated goat anti-mouse IgG1, IgG2a, IgG2b, or IgG3 (Novus Biological). Staining of all sections was visualized with a fluorescence microscope (BZ-8000; Keyence) using a plan Apo 20x NA0.75 lens. Immunofluorescence intensity (measured as the number of pixels/μm^2) was quantified using BZ analyzer II image analysis software (version 1.31; Keyence). At least 10 glomeruli per section were analyzed.

The most severely affected hind paw of each mouse was removed and fixed in 10% formalin. After decalcification in 10% EDTA, the joints were embedded in paraffin, and 4-μm–thick sections were stained with H&E and toluidine blue as described previously (38). In brief, twenty 4-μm sagittal serial sections were cut, every fifth section was stained with H&E, and an adjacent section was stained with toluidine blue. Histopathologic scoring was performed using a semiquantitative score, as described previously (39). The final histopathologic arthritis score was evaluated in each mouse by calculating the sum values for inflammation: infiltration of leukocytes, synovial hyperplasia, and destruction of cartilage, including pannus formation and cartilage erosion.

Four-micrometer paraffin-embedded sections of lipogranulomas from the peritoneal cavity as well as sections from the spleen and lymph nodes were deparaffinized, rehydrated, subjected to inhibition of endogenous peroxidase, and incubated with Blocking One Histo (Nacalai Tesque). They were then incubated with a purified anti-mouse Gal-9 antibody (BioLegend) overnight at 4°C, followed by goat anti-rat IgG conjugated with horseradish peroxidase (Abcam) for 1 hour, and developed with diaminobenzidine (SK-4100; Vector) as the chromogen. Sections were counterstained with Mayer's hematoxylin.

Quantitative real-time reverse transcription–polymerase chain reaction (RT-PCR). Mice were euthanized at 7 months after pristane injection, and the paws were then cut under the furline, unskinned, and immediately flash frozen in liquid nitrogen. Individual lipogranulomas were picked from the peritoneal cavity of pristane-injected mice and pooled. Paws and lipogranulomas were disrupted and homogenized in TRIzol reagents with a TOMY Micro Smash MS-100R and 5.5-mm stainless steel beads. The homogenates were centrifuged for 10 minutes at 4°C at 14,000 revolutions per minute. Supernatants were transferred to 1.5-ml Eppendorf tubes, centrifuged for 10 minutes at 4°C at 14,000 rpm, and collected for RNA extraction.

Total RNA was extracted from the paws, lipogranulomas, and peritoneal macrophages using an RNeasy Mini kit (Qiagen). Complementary DNA (cDNA) was generated using a High-Capacity cDNA RT kit (Applied Biosystems). Quantitative real-time PCR was performed in a Step One Plus Real-Time PCR system (Applied Biosystems) with specific primers, Universal Master Mix II (Life Technologies), and TaqMan gene expression assays to evaluate the expression of *Tnf* (Mm00443258_m1), *Il1b* (Mm00434228_m1), *Il6* (Mm00446190_m1), *Lgals1* (Mm00839408_g1), *Lgals9* (Mm00495295_m1), *Lgals3* (Mm00802901_m1), *Tlr3* (Mm01207404_m1), *Tlr4* (Mm00445273_m1), *Tlr7* (Mm00446590_m1), *Tlr9* (Mm00446193_m1), *Ccl2* (Mm00441242_m1), *Ccl7* (Mm00443113_m1), *Ccl12* (Mm01617100_m1), *Mx1* (Mm00487796_m1), *Cxcl10* (Mm00445235_m1), and *Irf7* (Mm00516793_g1). The relative abundance of mRNAs was standardized against the levels of *Gapdh* mRNA (Mm99999915_g1) as the invariant control.

Flow cytometry analysis. The spleen, mesenteric, and axillary lymph nodes from MRL/lpr mice were finely minced and incubated in a fresh digestion medium containing 3 ml RPMI 1640 with 2 mg/ml collagenase D (Roche), 50 IU DNase (Takara), and 10% fetal calf serum (FCS) at 37°C for 30 minutes, with gentle shaking at 200 rpm on an orbital shaker. Single-cell suspensions were prepared from the spleens and peritoneal lavage of PI mice, and from the lymph nodes of MRL/lpr mice. Red blood cells were removed using a red cell lysing buffer (BD Pharm Lyse). The cells were first incubated at 4°C for 10 minutes with an Fc receptor (FcR) blocking reagent (Miltenyi Biotec) to reduce nonspecific binding of antibodies to FcRs. The cells (1×10^6) derived from the spleen, peritoneum, and lymph nodes were incubated at 4°C for 30 minutes in staining buffer (BioLegend) with the relevant optimized amount of fluorochrome-conjugated antibodies or the appropriate isotype controls: FITC-conjugated anti-CD4 (GK1.5), VioBlue-conjugated anti-CD4 (GK1.5), allophyocyanin (APC)–conjugated anti-CD8 (53-6.7), APC-conjugated anti-CD62L (MEL14-H2.100), phycoerythrin (PE)–conjugated anti-CD44 (IM7.8.1), APC-conjugated anti-CD19 (6D5), FITC-conjugated anti-CD45R (B220) (RA3-6B2), APC-conjugated anti–Ly-6C (1G7.G10), PE-conjugated anti-CD138 (clone REA104), and PE-conjugated anti–Ly-6G (clone 1G7.G10). All antibodies were purchased from Miltenyi Biotec except BV421-conjugated anti-CD3 (SK7), which was purchased from BD Biosciences, and eFluor 450–conjugated anti-CD11b (M1/70), which was purchased from eBioscience. Dead cells were excluded from the analysis using 7-aminoactinomycin D staining (BD PharMingen). All data were acquired with a FACSAria I flow cytometer (BD Biosciences) and analyzed using FlowJo software (TreeStar).

In vitro assays of peritoneal macrophages. Peritoneal macrophages were harvested 24 hours after the injection of either pristane or phosphate buffered saline (PBS) as a vehicle control. The cells were seeded at a concentration of 1×10^6/well in UpCell 24-well plates (CellSeed) in Dulbecco's modified Eagle's medium supplemented with 10% FCS and 100 IU/ml penicillin/streptomycin, and incubated for 2 hours at 37°C in an atmosphere of 5% CO_2. Nonadherent cells were removed by washing with warm medium, and then recounted to calculate the number of adherent cells in the wells by subtraction. The remaining adherent cells consisted of >95% macrophages, and adherent macrophages were then cultured in the presence or absence of Toll-like receptor (TLR) ligands as described previously (40), or underwent protein extraction using Cell Lytic M reagent (Sigma-Aldrich) following the manufacturer's instructions. All ligands were purchased from InvivoGen except for lipopolysaccharide (Sigma-Aldrich). The supernatants were collected after 24 hours, and RNA was extracted and stored at −80°C.

Enzyme-linked immunosorbent assays (ELISAs). Serum levels of total IgG (Abcam), anti–double-stranded DNA (anti-dsDNA) (Shibayagi, Japan), anti–nuclear RNP (anti-nRNP) (Alpha Diagnostic International), and TNF (R&D Systems) were measured using commercially available ELISA kits according to the manufacturer's instructions. The cutoff values of the assays were 7.8 ng/ml, 15.6 mU/ml, 50 units/ml, and 10.9 ng/ml, respectively.

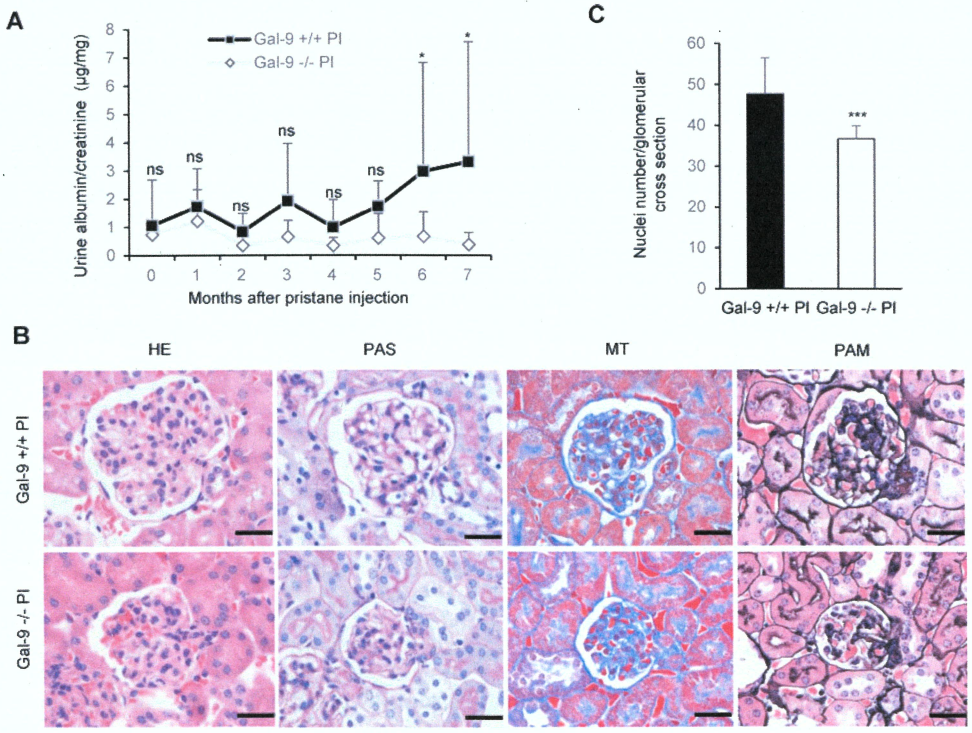

Figure 1. Attenuation of lupus nephritis in galectin 9–deficient (Gal-$9^{-/-}$) pristane-injected (PI) BALB/c mice. **A,** Levels of proteinuria in Gal-$9^{-/-}$ PI mice (n = 12) compared to Gal-$9^{+/+}$ PI mice (n = 11). **B,** Representative kidney sections from Gal-$9^{+/+}$ and Gal-$9^{-/-}$ PI mice, stained with hematoxylin and eosin (H&E), periodic acid–Schiff (PAS), Masson's trichrome (MT), and periodic acid–methenamine silver (PAM) for analysis of glomerular size and mesangial expansion. Bars = 30 µm. **C,** Numbers of glomerular nuclei in Gal-$9^{+/+}$ PI mice compared to Gal-$9^{-/-}$ PI mice (n = 10 per group). Results are the mean ± SD. * = $P < 0.05$; *** = $P < 0.001$, by Mann-Whitney U test in **A** and Student's *t*-test in **C**. NS = not significant.

Western blotting. For protein extraction, the tissue samples were homogenized in ice-cold radioimmunoprecipitation assay buffer. Total protein was quantified using the Pierce Protein Assay kit with Coomassie blue staining (using the Bradford) method according to the manufacturer's instructions (ThermoFisher Scientific). A Mini-PROTEAN precast gel (Bio-Rad) was equally loaded with 8.5 μg of protein, and then electrophoresed and electrotransferred to a PVDF membrane. After blocking with 5% nonfat dry milk and TBS-T (0.05% Tween 20, 20 m*M* Tris HCl, and 150 m*M* NaCl [pH 7.6]), membranes were probed with a primary antibody rat anti-mouse Gal-9 clone (clone 108A2; BioLegend) or rabbit anti-mouse GAPDH (Cell Signaling Technology), and then incubated with anti-rat IgG conjugated with horseradish peroxidase (Abcam) or donkey anti-rabbit IgG conjugated with horseradish peroxidase (Santa Cruz Biotechnology), respectively. Blots were developed using a Pierce ECL Plus Western blotting substrate and visualized using an ImageQuant LAS 4000 Mini kit (GE Healthcare Life Sciences).

Statistical analysis. Data are expressed as the mean ± SD. Normal distribution of the data was assessed by Shapiro-Wilk test, and statistically significant differences between groups were determined using the Student's 2-tailed t-test or Mann-Whitney U test, as appropriate. The incidence of arthritis was analyzed using a Fisher's exact test. Data were analyzed using JMP 13 software (SAS). *P* values less than 0.05 were considered significant.

RESULTS

Attenuation of pristane-induced lupus nephritis in *Lgals9*-deficient mice. Pristane induces immune complex glomerulonephritis in BALB/c mice, a condition that is associated with the same autoantibodies typically observed in human SLE (28). Gal-$9^{-/-}$ PI mice (pristane-injected BALB/c mice) developed only modest proteinuria compared to Gal-$9^{+/+}$ PI mice (Figure 1A). Furthermore, light microscopic examination of the tissue sections demonstrated an attenuation of histologic damage in Gal-$9^{-/-}$ PI mice, as evidenced by a reduction in glomerular size, reduced cellularity, and suppression of mesangial expansion (Figures 1B and C).

We also assessed the effect of Gal-9 deficiency on glomerular immune complex formation/deposition. Kidney sections from Gal-$9^{-/-}$ and Gal-$9^{+/+}$ PI mice were stained for IgG and C3 at 7 months after pristane injection. As evident on the representative glomerular sections shown in Figure 2A, we found a significant reduction in the glomerular immune complex deposition of IgG, all of the IgG subclasses, and C3 in Gal-$9^{-/-}$ PI mice compared to their Gal-$9^{+/+}$ littermates.

In contrast, no differences with regard to kidney involvement between Gal-$9^{-/-}$ MRL/lpr mice and Gal-$9^{+/+}$ MRL/lpr mice were seen when measured as either albuminuria, glomerular hypercellularity, or tubulointerstitial disease (for results, see Supplementary Figures 2A–C, available on the *Arthritis & Rheumatology* web site at http://onlinelibrary.wiley.com/doi/10.1002/art.40467/abstract). Active pathologic features such as cellular crescents, wire loop formation, hyaline thrombi, and glomerular necrosis were similar between Gal-$9^{-/-}$ MRL/lpr mice and Gal-$9^{+/+}$ MRL/lpr mice (see Supplementary Figure 2D, http://onlinelibrary.wiley.com/doi/10.1002/art.40467/abstract).

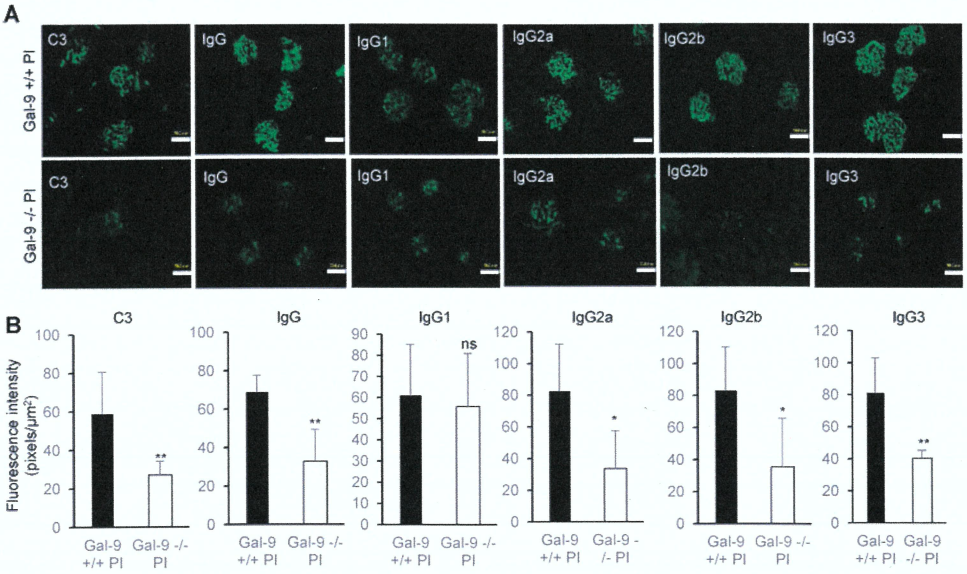

Figure 2. Reduced glomerular IgG deposition in Gal-$9^{-/-}$ PI mice. **A,** Deposition of C3, IgG, and IgG subclasses, as evaluated by direct immunofluorescence, in the kidneys from Gal-$9^{-/-}$ PI mice compared to Gal-$9^{+/+}$ PI mice. Images are representative of 5 mice per group. Bars = 50 μm. **B,** Immunofluorescence intensity of C3, IgG, and IgG-subclass deposits, as evaluated using computed image analysis software. The final fluorescence intensity score reflects the average of at least 10 glomeruli per mouse. Results are the mean ± SD. * = $P < 0.05$; ** = $P < 0.01$, by Student's *t*-test. See Figure 1 for definitions.

Furthermore, there were no alterations or reductions in immune complex deposition in Gal-9$^{-/-}$ MRL/lpr mice as compared to Gal-9$^{+/+}$ MRL/lpr littermates (see Supplementary Figures 2E and F, http://onlinelibrary.wiley.com/doi/10.1002/art.40467/abstract). These results suggest that Gal-9 deficiency is capable of suppressing the functional and pathologic damage to the kidneys induced by pristane injection, but it is not sufficient to prevent severe forms of kidney disease associated with impaired apoptosis/cell clearance in MRL/lpr mice.

Pristane-induced production of IgG and autoantibodies in Gal-9$^{-/-}$ BALB/c mice. Hypergammaglobulinemia and autoantibody production against a broad range of autoantigens are characteristic features of pristane-induced lupus in BALB/c mice (29,41,42). To evaluate the impact of *Lgals9* deficiency on pristane-induced hypergammaglobulinemia and autoantibody production, serum was collected at baseline and every month after pristane injection for 7 months. Serum levels of total IgG were significantly lower in Gal-9$^{-/-}$ PI mice compared to Gal-9$^{+/+}$ PI mice (Figure 3A). Body weight, spleen weight, and the total number of splenocytes were not altered in either Gal-9$^{-/-}$ or Gal-9$^{+/+}$ PI mice (for results, see Supplementary Figures 3A–C, available on the *Arthritis & Rheumatology* web site at http://onlinelibrary.wiley.com/doi/10.1002/art.40467/abstract). Flow cytometry analysis of the spleens and peritoneal lavage did not reveal any differences in the numbers of B cells and plasma cell subsets (Supplementary Figures 3D–F, http://onlinelibrary.wiley.com/doi/10.1002/art.40467/abstract).

We next investigated the titers of anti-nRNP and anti-dsDNA, both of which are hallmarks of SLE and have been previously found in 50–90% and 40% of pristane-treated BALB/c mice, respectively (29). The titers of anti-dsDNA and anti-nRNP antibodies were increased both in Gal-9$^{-/-}$ PI mice and in Gal-9$^{+/+}$ PI mice, but their titers were comparable between the 2 groups (Figures 3B and C). In Gal-9$^{-/-}$ and Gal-9$^{+/+}$ MRL/lpr mice, there were no statistically significant differences in the levels of anti-dsDNA antibodies (for results, see Supplementary Figure 2G, http://onlinelibrary.wiley.com/doi/10.1002/art.40467/abstract).

Body weights, spleen weights, lymph node weights, and total cell numbers in the spleen and lymph nodes were not altered in either Gal-9$^{-/-}$ or Gal-9$^{+/+}$ MRL/lpr mice (for results, see Supplementary Figures 4A–D, available on the *Arthritis & Rheumatology* web site at http://onlinelibrary.wiley.com/doi/10.1002/art.40467/abstract). Flow cytometry analysis of the spleen and lymph nodes did not reveal any differences in the numbers of B cells and T cell subsets, except that there was a reduction in the number of double-negative T cells in the spleens of Gal-9$^{-/-}$ MRL/lpr mice (see Supplementary Figures 4D–G, http://onlinelibrary.wiley.com/doi/10.1002/art.40467/abstract). Although deficiency of Gal-9 suppressed overall production of IgG in these mice, it did not diminish the production of pathogenic plasma cells producing antibodies against autoantigens.

Amelioration of arthritis in Gal-9$^{-/-}$ PI mice. A single injection of pristane into the peritoneal cavity induces an erosive arthritis in susceptible mouse strains such as BALB/cJ mice (30). In the present study, the incidence of arthritis increased over time and was higher in Gal-9$^{+/+}$ PI mice (72%) than in Gal-9$^{-/-}$ PI mice (33%) (Figure 4A). At 7 months after pristane injection, the mean clinical arthritis severity score was significantly reduced in Gal-9$^{-/-}$ PI mice compared to Gal-9$^{+/+}$ PI mice (Figure 4B). These results indicate that *Lgals9* deficiency fully protects against arthritis development in mice, and reduces the severity of arthritis in affected mice.

The extent of joint destruction and severity of inflammation were evaluated by H&E and toluidine blue staining of the joint sections. Synovial hyperplasia, severe leukocyte infiltration, pannus formation, and cartilage

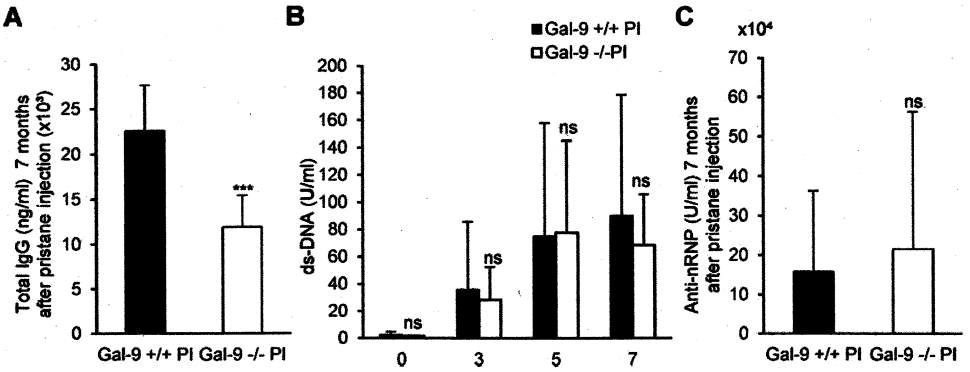

Figure 3. Hypergammaglobulinemia and autoantibody production in Gal-9$^{+/+}$ and Gal-9$^{-/-}$ PI mice. Serum levels of total IgG at 7 months following pristane injection (n = 8 mice per group) **(A)**, double-stranded DNA (dsDNA) antibodies at 0, 3, 5, and 7 months postinjection (n = 6 mice per group) **(B)**, and anti–nuclear RNP (anti-nRNP) antibodies at 7 months postinjection (n = 7 mice per group) **(C)** were measured by enzyme-linked immunosorbent assay in Gal-9$^{+/+}$ and Gal-9$^{-/-}$ PI mice. Results are the mean ± SEM in duplicate samples. *** = $P < 0.001$, by Student's *t*-test. See Figure 1 for other definitions.

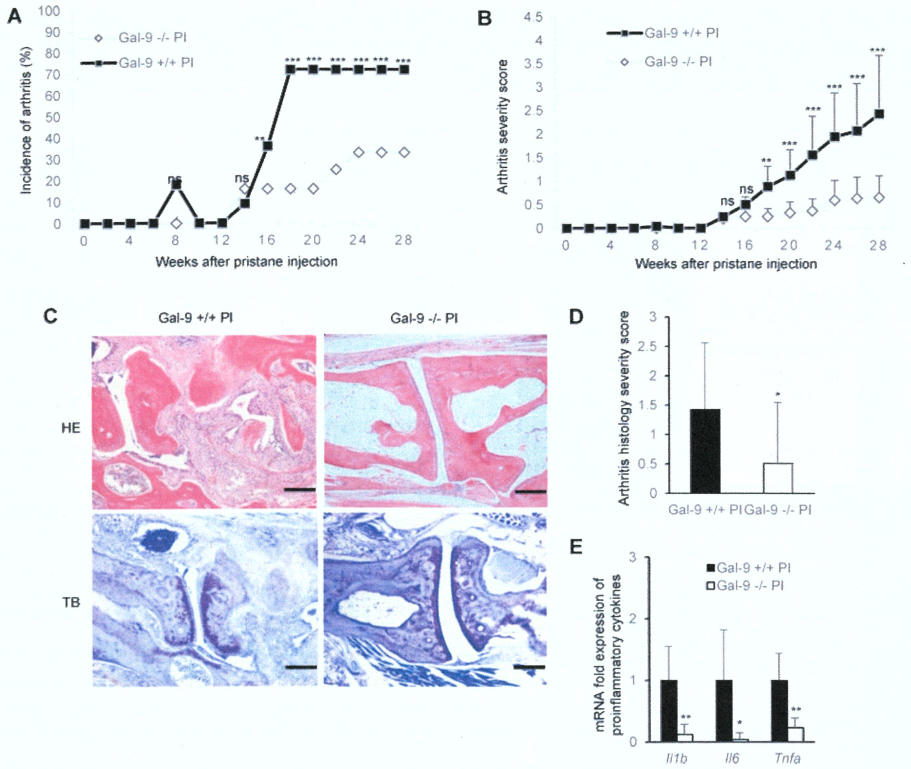

Figure 4. Incidence and severity of pristane-induced arthritis in Gal-$9^{-/-}$ and Gal-$9^{+/+}$ mice. **A,** Incidence of arthritis in Gal-$9^{-/-}$ PI mice (n = 12) compared to Gal-$9^{+/+}$ PI mice (n = 11), calculated as the percentage of mice that developed redness or swelling in at least 1 paw among all mice in each group. **B,** Mean clinical arthritis severity score in Gal-$9^{+/+}$ PI mice (n = 11) compared to Gal-$9^{-/-}$ PI mice (n = 12). The arthritis severity score (scale of 0–3) evaluated the severity of erythema/swelling in the wrist or ankle. **C,** Histopathologic evaluation of arthritis by staining of the joints with H&E and toluidine blue (TB). Representative histopathologic sections of the joints from Gal-$9^{+/+}$ and Gal-$9^{-/-}$ PI mice are shown. Bars = 30 μm. **D,** Semiquantitative histologic scoring of arthritis. Sections of the joints from Gal-$9^{-/-}$ PI and Gal-$9^{+/+}$ PI mice (n = 10 per group) were stained with H&E and TB and evaluated for the extent of inflammation and joint destruction. **E,** Determination of cytokine mRNA expression in the joints of Gal-$9^{+/+}$ PI mice compared to Gal-$9^{-/-}$ PI mice (n = 6 per group). Expression levels of *Il1b*, *Il6*, and *Tnfa* were assessed by reverse transcription–polymerase chain reaction. Results are the mean ± SD. * = $P < 0.05$; ** = $P < 0.01$; *** = $P < 0.001$, by Fisher's exact test in **A** and **B** and by Student's *t*-test in **D** and **E**. See Figure 1 for other definitions.

erosions were present in the joints of Gal-$9^{+/+}$ PI mice, whereas the joints of Gal-$9^{-/-}$ PI mice were largely spared, showing marked reductions in the extent of synovitis and severity of joint erosion (Figure 4C). The histopathologic arthritis severity scores were significantly lower in Gal-$9^{-/-}$ PI mice than in Gal-$9^{+/+}$ PI mice (Figure 4D). In addition, *Lgals9* deficiency reduced the expression of mRNA for several proinflammatory cytokines, including *Il1b*, *Il6*, and *Tnfa*, in Gal-$9^{-/-}$ PI mice compared to Gal-$9^{+/+}$ PI mice (Figure 4E).

Altered chronic peritoneal inflammatory response in Gal-$9^{-/-}$ PI mice. The pristane-induced lupus model is characterized by lipogranuloma formation, which is a chronic inflammatory response to the hydrocarbon oil and has morphologic and functional characteristics of secondary lymphoid tissue (43,44). At 7 months after pristane injection, numerous lipogranulomas were observed in the peritoneal cavity of Gal-$9^{+/+}$ PI mice, whereas lipogranulomas were markedly reduced in number and size in Gal-$9^{-/-}$ PI mice (Figure 5A) and were completely absent in 2 of 12 Gal-$9^{-/-}$ PI mice (data not shown).

Intriguingly, H&E staining of the lipogranulomas demonstrated a smaller size, diminished cellularity, and absence of follicle-like structures in Gal-$9^{-/-}$ PI mice compared to Gal-$9^{+/+}$ PI mice (Figure 5A). The number of high endothelial venules (HEVs) was reduced in Gal-$9^{-/-}$ PI mice compared to Gal-$9^{+/+}$ PI mice (for results, see Supplementary Figure 5A, available on the *Arthritis & Rheumatology* web site at http://onlinelibrary.wiley.com/doi/10.1002/art.40467/abstract). The smaller oil droplets were surrounded by inflammatory cells and uniformly distributed in the lipogranulomas of Gal-$9^{+/+}$ PI mice, whereas larger oil droplets were eccentrically located and surrounded by fibrotic tissue (Figure 5A).

Moreover, Gal-9 was found to be distributed mainly in areas surrounding the follicle-like structure in lipogranulomas, the lymphoid follicle of the lymph nodes, and the marginal zone of the spleen (Figure 5B). RT-

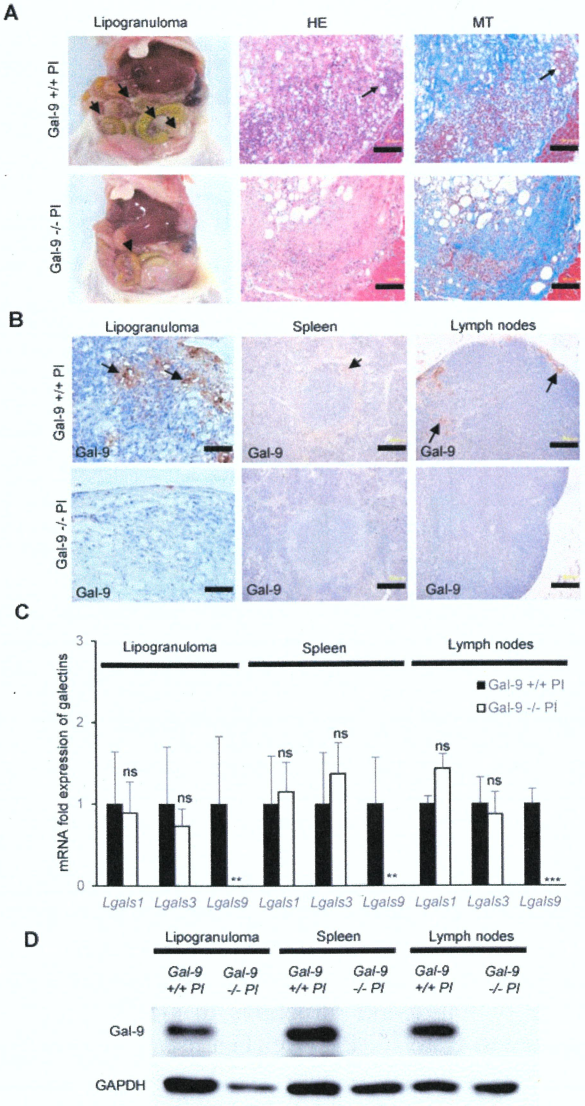

Figure 5. Reduction in the peritoneal inflammatory response in Gal-$9^{-/-}$ PI mice. **A,** Frequency of lipogranulomas in the peritoneal cavity of a Gal-$9^{-/-}$ PI mouse compared to a Gal-$9^{+/+}$ PI mouse. Left, Histopathologic sections were assessed for the presence of lipogranulomas. Differences between the 2 groups were characterized by differences in the size of the oil droplets, cells, and matrix distribution. Middle and Right, Sections of ectopic lymphoid tissue were stained with H&E and MT at 7 months after pristane injection. Bars = 20 μm. Representative samples are shown. **B,** Immunohistologic staining for the expression of Gal-9 in the lipogranulomas, spleen, and lymph nodes of a Gal-$9^{+/+}$ PI mouse compared to a Gal-$9^{-/-}$ PI mouse. Bars = 50 μm. In **A** and **B**, **arrows** indicate follicle-like structures. **C,** Expression levels of *Lgals* mRNA in the lipogranulomas, spleen, and lymph nodes of Gal-$9^{+/+}$ PI mice compared to a Gal-$9^{-/-}$ PI mice (n = 6 per group). Results are the mean ± SD. ** = $P < 0.01$; *** = $P < 0.001$, by Student's *t*-test. **D,** Representative Western blots of Gal-9 expression in the lipogranulomas, spleen, and lymph nodes of a Gal-$9^{+/+}$ PI mouse compared to a Gal-$9^{-/-}$ PI mouse; GAPDH was used as the invariant control. See Figure 1 for definitions.

PCR and Western blot analyses demonstrated that *Lgals9* mRNA was highly expressed in the lipogranulomas, spleens, and lymph nodes of Gal-$9^{+/+}$ PI mice and absent in Gal-$9^{-/-}$ PI mice (Figures 5C and D). There was no compensatory up-regulation of *Lgals1* and *Lgals3* mRNA in Gal-$9^{-/-}$ PI mice. These results suggest that Gal-9 is essentially required for the neogenesis of tertiary lymphoid tissue in response to pristane in vivo.

Effects of *Lgals9* deficiency on the innate immune response of peritoneal macrophages. Peritoneal macrophages are the foremost cells that sense and interact with pristane following its injection. As a result, they release a wide range of proinflammatory cytokines and chemokines in the peritoneal cavity, followed by accumulation of inflammatory Ly-$6C^{high}$ monocytes, the main source of type I interferons (IFNs) in this model (45). We thus examined the effect of *Lgals9* deficiency on cellular composition in the spleen and peritoneal lavage cells at 15 days and 7 months after pristane injection. We observed no alterations in the frequency of T cells, B cells, effector/memory CD4+ T cells, and CD11b cells in Gal-$9^{-/-}$ PI mice compared to Gal-$9^{+/+}$ PI mice (results in Supplementary Figure 3D, http://onlinelibrary.wiley.com/doi/10.1002/art.40467/abstract). At 15 days after pristane injection, the recruitment of CD11b+Ly-$6C^{high}$ inflammatory monocytes into the peritoneal cavity was not impaired in Gal-$9^{-/-}$ PI mice (results in Supplementary Figure 3G, http://onlinelibrary.wiley.com/doi/10.1002/art.40467/abstract).

We then isolated peritoneal macrophages at 24 hours after pristane injection and cultured the cells for gene expression analyses. The peritoneal macrophages from Gal-$9^{-/-}$ PI mice demonstrated reduced *Tnfa* mRNA expression in response to pristane as compared to Gal-$9^{+/+}$ PI mice, and transcriptional activities of *Il1 and Il6* were not affected (Figure 6A). Moreover, *Lgals9* deficiency did not affect the expression of TLRs in peritoneal macrophages following pristane injection (Figure 6A). Such an effect appeared to be pristane-dependent, since the isolated and cultured peritoneal macrophages from PBS-injected Gal-$9^{-/-}$ mice did not show any significant up-regulation of *Il1b*, *Il6*, or *Tnfa* mRNA as compared to PBS-injected Gal-$9^{+/+}$ mice (Figure 6B). Although the expression of *Tnfa* mRNA was reduced in Gal-$9^{-/-}$ PI mice compared to their Gal-$9^{+/+}$ PI littermates, there were no significant differences in the TNF protein concentrations in the supernatants of cultured peritoneal macrophages from these mice (Figure 6C).

We also investigated time-course changes in *Tnfa* expression at 4, 24, and 48 hours after pristane injection, and TNF protein concentrations at 24 and 48 hours, in the isolated peritoneal macrophages without culture. Again, there were no significant differences in *Tnfa* mRNA expression between Gal-$9^{-/-}$ PI mice and Gal-$9^{+/+}$ PI mice (Figures 6D and E).

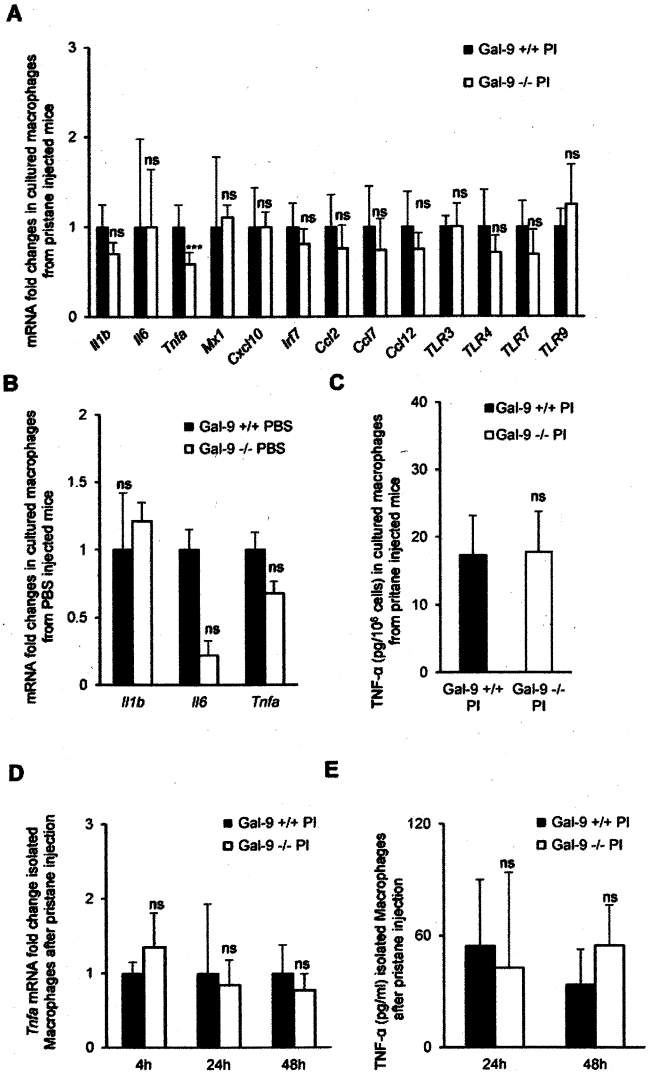

Figure 6. Expression of cytokines and Toll-like receptors (TLRs) in mouse peritoneal macrophages primed with pristane injection. **A,** Fold change in expression of mRNA for *Il1b, Il6, Tnfa,* interferon (IFN)–stimulated genes, type I IFN–induced chemokines, and TLRs was assessed by reverse transcription–polymerase chain reaction (RT-PCR) at 24 hours after pristane injection in peritoneal macrophages from Gal-$9^{-/-}$ PI mice compared to Gal-$9^{+/+}$ PI mice (n = 5 per group). **B,** Fold change in expression of mRNA for *Il1b, Il6,* and *Tnfa* was assessed in Gal-$9^{-/-}$ and Gal-$9^{+/+}$ mice (n = 3 per group) at 24 hours after phosphate buffered saline (PBS) injection. **C,** Production of tumor necrosis factor (TNF) was measured by enzyme-linked immunosorbent assay (ELISA) in culture supernatants of peritoneal macrophages from Gal-$9^{-/-}$ PI mice compared to Gal-$9^{+/+}$ PI mice (n = 5 per group) at 24 hours after pristane injection. **D,** Fold change in expression of mRNA for *Tnfa* was assessed by RT-PCR at 4 hours, 24 hours, and 48 hours after pristane injection in peritoneal macrophages from Gal-$9^{-/-}$ PI mice compared to Gal-$9^{+/+}$ PI mice (n = 4 per group). **E,** Production of TNF was measured by ELISA in cell lysates of peritoneal macrophages from Gal-$9^{-/-}$ PI mice compared to Gal-$9^{+/+}$ PI mice (n = 4 per group) at 24 hours and 48 hours after pristane injection. Results are the mean ± SD. *** = $P <$ 0.001 by Student's *t*-test. See Figure 1 for other definitions.

We further analyzed the response of peritoneal macrophages to various TLR ligands. Unexpectedly, after stimulation of peritoneal macrophages with TLR ligands for 24 hours, positive effects of the TLR-3, TLR-4, and TLR-9 ligands on *Tnfa* gene expression were observed in the peritoneal macrophages from mice with *Lgals9* deficiency, with statistically significant differences compared to Gal-$9^{+/+}$ PI mice (for results, see Supplementary Figures 6A, B, and D, available on the *Arthritis & Rheumatology* web site at http://onlinelibrary.wiley.com/doi/10.1002/art.40467/abstract), whereas the TLR-7 ligand did not exert a stimulatory effect on *Tnfa* mRNA expression (see Supplementary Figure 6C, http://onlinelibrary.wiley.com/doi/10.1002/art.40467/abstract). Furthermore, stimulation with TLR ligands did not alter *Tnfa* mRNA expression, nor did it alter supernatant TNF concentrations, in cultured peritoneal macrophages from PBS-injected Gal-$9^{-/-}$ mice compared to PBS-injected Gal-$9^{+/+}$ mice (see Supplementary Figures 6E and F, http://onlinelibrary.wiley.com/doi/10.1002/art.40467/abstract). These results suggest that *Lgals9* deficiency does not alter the pristane-induced recruitment of inflammatory leukocytes into the peritoneal cavity, nor does it impair the sensitivities of cytokine production stimulated by TLR ligands.

Role of *Lgals9* deficiency in conferring protection against pristane-induced lupus in a manner independent of the TLR-7–type I IFN pathway. The activation of the TLR-7/myeloid differentiation factor 88 pathway triggers the subsequent secretion of type I IFN and the expression of IFN-stimulated genes (ISGs) and chemokines. Since TLR-7–type I IFN is the essential pathway for the development of pristane-induced lupus (46), we investigated whether *Lgals9* deficiency protected against the development of pristane-induced lupus via alterations in the TLR-7–type I IFN pathway in peritoneal macrophages. The expression levels of ISGs (*Mx1, Cxcl10,* and *Irf7*) and IFN-induced chemokines (*Ccl2, Ccl7,* and *Ccl12*) in the peritoneal macrophages were comparable between Gal-$9^{-/-}$ PI mice and Gal-$9^{+/+}$ PI mice (Figure 6A). In cultured peritoneal macrophages, there was no difference in the expression of ISGs and IFN-induced genes stimulated with various TLR ligands between Gal-$9^{-/-}$ PI mice and Gal-$9^{+/+}$ PI mice (see Supplementary Figures 5A–D, http://onlinelibrary.wiley.com/doi/10.1002/art.40467/abstract). These results suggest that *Lgals9* deficiency does not alter the TLR-7–type I IFN pathway in the peritoneal macrophages of mice with pristane-induced lupus.

DISCUSSION

It has been postulated that the application of exogenous Gal-9 may limit the pathogenic activities of T

cells, such as the activation of Th1 and Th17 cells (19). Indeed, the therapeutic effect of recombinant Gal-9 has been successfully demonstrated in several autoimmune disease models, including CIA (20,33), immune complex–induced arthritis (47), and spontaneous lupus in MRL/lpr mice (24). We initially hypothesized that *Lgals9* deficiency would exacerbate the clinical features of SLE in pristane-injected BALB/c mice and in the MRL/lpr mouse model of lupus. However, unexpectedly, *Lgals9* deficiency significantly ameliorated glomerulonephritis, arthritis, and lipogranuloma formation in pristane-injected BALB/c mice, whereas in MRL/lpr mice, glomerulonephritis and lymphadenopathy were not altered. Although many researchers have attempted to explore the clinical application of recombinant Gal-9 in autoimmune diseases, the development of antagonists to Gal-9 is also a new option in the treatment of autoimmune diseases. The small molecules that interfere with the binding between β-galactoside and Gal-9 may be such candidates for therapy. Human recombinant Gal-9 lacking a link peptide, designated hG9NC (null), is more resistant to proteolysis in the serum, limits lattice formation by reduced rotational freedom of carbohydrate binding domains (CRDs), and also works as an antagonist against the CRD-dependent effects of native Gal-9 (16).

Lgals9 deficiency did not alter the production of autoantibodies in either pristane-injected BALB/c mice or MRL/lpr mice, and anti-nRNP and anti-dsDNA antibodies were equally present in Gal-$9^{-/-}$ PI mice and Gal-$9^{+/+}$ PI mice. There was no impairment in the development of B cells and maturation to plasma cells, suggesting that Gal-9 is not required for autoantibody production, nor was B cell differentiation impaired in antibody-secreting cells. Although Gal-9 induces the differentiation of naive T cells to Treg cells and suppresses differentiation to Th1 and Th17 cells in in vitro experiments (20), we found no alterations of cell populations in lymphocytes from the spleen and peritoneal lavage between Gal-$9^{-/-}$ PI mice and Gal-$9^{+/+}$ PI mice. Double-negative T cells are known to expand and stimulate autoantibody production by secreting IL-17 and IFNγ (48), and reductions in the number of double-negative cells were observed in the spleens of Gal-$9^{-/-}$ MRL/lpr mice; however, we did not observe a reduction in autoantibody production.

In contrast to that seen in the spleen and lymph nodes, a significant reduction in lipogranuloma formation was observed in Gal-$9^{-/-}$ PI mice. Lipogranulomas induced by pristane injection consisted of B cells, CD4+ T cells, and DCs. Lipogranulomas are regarded as a form of ectopic lymphoid tissue, i.e., tertiary lymphoid tissue (44). The mechanism of lipogranuloma formation remains largely unknown, but presumably the recruitment of inflammatory cells in response to different chemokines and cytokines triggered by pristane injection plays a crucial role in the development of this unique structure. There was no impairment in leukocyte recruitment into the peritoneal cavity of Gal-$9^{-/-}$ PI mice; however, the formation and development of lipogranulomas was prominently diminished, and even completely absent, in some Gal-$9^{-/-}$ PI mice. Although the formation and development of lipogranulomas was not initially altered in Gal-$9^{-/-}$ PI mice, they might undergo resolution through the reduction in cellular maintenance and supply that occurs as result of the reduced number of HEVs, or through the reduction in pristane-induced cytokine production in the peritoneal cavity over time. The injection of pristane into the peritoneal cavity triggers an inflammatory local response characterized by the priming and activation of peritoneal macrophages (27), which results in the production of an array of inflammatory cytokines and chemokines, an enhanced stimulation by TLRs, and the recruitment, infiltration, and activation of inflammatory cells operating the innate and adaptive immune system in the peritoneal cavity.

We initially hypothesized that the ameliorated arthritis and glomerulonephritis in our model could be attributed to an impairment in the recruitment of inflammatory leukocytes into the peritoneal cavity, but Gal-9 deficiency did not affect the recruitment of inflammatory leukocytes into the peritoneal cavity. It is well-known that Gal-9 enhances TNF secretion in DCs (15,49) and microglial cells (50), belonging to the monocytic lineage. The interaction of TLRs and TLR ligands links to the common downstream signaling pathway, but their interaction produces different amounts or types of cytokines in the same cell, due in part to the quantitative and qualitative nature of the interaction between the TLRs and their ligand (51). Thus, we extensively investigated the basal and stimulated production of TNF protein by various TLR ligands, such as TLR-3, TLR-4, TLR-7, and TLR-9, in cultured peritoneal macrophages. In Gal-$9^{-/-}$ PI mice, the basal and TLR ligand–stimulated production of TNF protein from the peritoneal macrophages was not altered, although a certain degree of reduction in expression of *Tnfa* transcripts in the basal condition, and hyperresponsiveness in stimulated conditions, was observed. It is known that several cytokine genes, including *Tnfa*, undergo posttranscriptional regulation at the mRNA and protein translational levels (52), and the overall and final output of TNF in response to pristane was not influenced by *Lgals9* deficiency.

As demonstrated by several studies, the mouse model of pristane-induced lupus is known to be

dependent on the TLR-7–type I IFN pathway. Type I IFN is induced by the Ly-6C^{high} subset of immature monocytes, and the animal model is characterized by an increased expression of type I IFN–induced genes, the so-called IFN signature (45,46,53). The sustained production of anti-nRNP antibodies is dependent on TLR-7 ligand stimulation in the switched memory-like B cell subset (54). In the current investigation, we found no defects or reductions in the expression of several ISGs and IFN-induced chemokines, accumulation of Ly-6C^{high} inflammatory monocytes in the peritoneal cavity, or production of anti-nRNP. Thus, *Lgals9* deficiency appears to protect against pristane-induced lupus in mice in a manner independent of the TLR-7–type I IFN pathway in peritoneal macrophages.

Based on the findings in the current study, we can speculate as to why mice are protected against pristane-induced lupus in this model, while MRL/lpr mice are not. The single-cell response of basal and pristane-primed peritoneal macrophages to TLR ligands was not altered by *Lgals9* deficiency, as evidenced by the findings with regard to production of TNF, type I IFN, ISGs, and IFN-induced chemokines. However, Gal-9 is essentially required for the neogenesis of tertiary lymphoid tissue, which is characterized by lymphoid follicle–like structures and HEVs in response to pristane in vivo, although the formation of lymphoid tissues, such as lymph nodes and spleen, was not impaired in Gal-9$^{-/-}$ mice. The Gal-9Δ5 splice variant was found to be highly expressed in endothelial cells in different tumors, and it enhanced sprouting and migration of human umbilical vein endothelial cells toward a Gal-9Δ5 gradient (55). HEVs are the major entry port for immune cells in secondary lymphoid organs (56), and the reduced cellularity observed in Gal-9$^{-/-}$ PI mouse lipogranulomas suggests that inflammatory cells could be recruited via these newly formed vessels. Moreover, Gal-9 deficiency could have hampered their recruitment by inhibiting the formation of HEVs.

Another explanation for the protection against pristane-induced lupus in this model would be that Gal-9 is essential for lipogranuloma formation since it modulates cell adhesion and cell cluster formation (57). Lipogranulomas consist of immune cell clusters, and Gal-9 deficiency may impair cell adhesion, resulting in reduced cell aggregation and lipogranuloma formation. The formation of tertiary lymphoid-like structures also requires signals provided by the local environment, together with an appropriate stromal response, where Gal-9 is highly expressed.

In summary, the current investigation in Gal-9$^{-/-}$ PI mice suggests that the antagonism of Gal-9 is beneficial for the treatment of nephritis and arthritis in SLE. *Lgals9* deficiency did not affect the survival and apoptosis of T and B cells nor did it affect the production of cytokines from peritoneal macrophages; however, it notably caused a reduction in lipogranuloma formation. The apoptotic potential of the Gal-9 recombinant protein is dose-dependent, and a lower dose of Gal-9 or decline in the concentration of Gal-9 may cause enhanced cytokine production. The current therapy for SLE, which includes steroids and immunosuppressant agents, is associated with severe infections, a complication that impairs the quality of life in patients with SLE. A more robust and vigorous virus-specific immune response to acute and chronic viral infections is mounted in Gal-9–deficient mice, resulting in rapid viral clearance. Thus, antagonism of Gal-9 signaling may be beneficial for the prevention of various infections, including viral infection (58), in patients with SLE.

AUTHOR CONTRIBUTIONS

All authors were involved in drafting the article or revising it critically for important intellectual content, and all authors approved the final version to be published. Dr. Wada had full access to all of the data in the study and takes responsibility for the integrity of the data and the accuracy of the data analysis.

Study conception and design. Zeggar, K. S. Watanabe, Wada.

Acquisition of data. Zeggar, K. S. Watanabe, Teshigawara, Hiramatsu, T. Katsuyama, E. Katsuyama, H. Watanabe, Matsumoto, Kawabata, Sada, Niki, Hirashima, Wada.

Analysis and interpretation of data. Zeggar, K. S. Watanabe, Hiramatsu, T. Katsuyama, E. Katsuyama, H. Watanabe, Matsumoto, Kawabata, Wada.

REFERENCES

1. Croca SC, Rodrigues T, Isenberg DA. Assessment of a lupus nephritis cohort over a 30-year period. Rheumatology (Oxford) 2011;50:1424–30.
2. Lateef A, Petri M. Unmet medical needs in systemic lupus erythematosus. Arthritis Res Ther 2012;14 Suppl 4:S4.
3. Tektonidou MG, Dasgupta A, Ward MM. Risk of end-stage renal disease in patients with lupus nephritis, 1971–2015: a systematic review and Bayesian meta-analysis. Arthritis Rheumatol 2016;68: 1432–41.
4. Van Vugt RM, Derksen RH, Kater L, Bijlsma JW. Deforming arthropathy or lupus and rhupus hands in systemic lupus erythematosus. Ann Rheum Dis 1998;57:540–4.
5. Bauernfeind B, Aringer M, Prodinger B, Kirchberger I, Machold K, Smolen J, et al. Identification of relevant concepts of functioning in daily life in people with systemic lupus erythematosus: a patient Delphi exercise. Arthritis Rheum 2009;61:21–8.
6. Wada J, Kanwar YS. Identification and characterization of galectin-9, a novel β-galactoside-binding mammalian lectin. J Biol Chem 1997;272:6078–86.
7. Wada J, Ota K, Kumar A, Wallner EI, Kanwar YS. Developmental regulation, expression, and apoptotic potential of galectin-9, a β-galactoside binding lectin. J Clin Invest 1997;99:2452–61.
8. Nio-Kobayashi J. Tissue- and cell-specific localization of galectins, β-galactose-binding animal lectins, and their potential functions in health and disease. Anat Sci Int 2017;92:25–36.

9. John S, Mishra R. Galectin-9: from cell biology to complex disease dynamics. J Biosci 2016;41:507–34.
10. Zhang ZY, Dong JH, Chen YW, Wang XQ, Li CH, Wang J, et al. Galectin-9 acts as a prognostic factor with antimetastatic potential in hepatocellular carcinoma. Asian Pac J Cancer Prev 2012;13:2503–9.
11. Kashio Y, Nakamura K, Abedin MJ, Seki M, Nishi N, Yoshida N, et al. Galectin-9 induces apoptosis through the calcium-calpain-caspase-1 pathway. J Immunol 2003;170:3631–6.
12. Lu LH, Nakagawa R, Kashio Y, Ito A, Shoji H, Nishi N, et al. Characterization of galectin-9-induced death of Jurkat T cells. J Biochem 2007;141:157–72.
13. Heusschen R, Griffioen AW, Thijssen VL. Galectin-9 in tumor biology: a jack of multiple trades. Biochim Biophys Acta 2013;1836:177–85.
14. Dai SY, Nakagawa R, Itoh A, Murakami H, Kashio Y, Abe H, et al. Galectin-9 induces maturation of human monocyte-derived dendritic cells. J Immunol 2005;175:2974–81.
15. Li Y, Feng J, Geng S, Geng S, Wei H, Chen G, et al. The N- and C-terminal carbohydrate recognition domains of galectin-9 contribute differently to its multiple functions in innate immunity and adaptive immunity. Mol Immunol 2011;48:670–7.
16. Fujita K, Iwama H, Oura K, Tadokoro T, Samukawa E, Sakamoto T, et al. Cancer therapy due to apoptosis: galectin-9. Int J Mol Sci 2017;18.
17. Zhu C, Anderson AC, Schubart A, Xiong H, Imitola J, Khoury SJ, et al. The Tim-3 ligand galectin-9 negatively regulates T helper type 1 immunity. Nat Immunol 2005;6:1245–52.
18. Gooden MJ, Wiersma VR, Samplonius DF, Gerssen J, van Ginkel RJ, Nijman HW, et al. Galectin-9 activates and expands human T-helper 1 cells. PLoS One 2013;8:e65616.
19. Wiersma VR, de Bruyn M, Helfrich W, Bremer E. Therapeutic potential of Galectin-9 in human disease. Med Res Rev 2013;33 Suppl 1:E102–26.
20. Seki M, Oomizu S, Sakata KM, Sakata A, Arikawa T, Watanabe K, et al. Galectin-9 suppresses the generation of Th17, promotes the induction of regulatory T cells, and regulates experimental autoimmune arthritis. Clin Immunol 2008;127:78–88.
21. Parker MH, Malone KH III, Trier AC, Striano TS. Evaluation of resistance form for prepared teeth. J Prosthet Dent 1991;66:730–3.
22. Katoh S, Ishii N, Nobumoto A, Takeshita K, Dai SY, Shinonaga R, et al. Galectin-9 inhibits CD44-hyaluronan interaction and suppresses a murine model of allergic asthma. Am J Respir Crit Care Med 2007;176:27–35.
23. Tsuchiyama Y, Wada J, Zhang H, Morita Y, Hiragushi K, Hida K, et al. Efficacy of galectins in the amelioration of nephrotoxic serum nephritis in Wistar Kyoto rats. Kidney Int 2000;58: 1941–52.
24. Moritoki M, Kadowaki T, Niki T, Nakano D, Soma G, Mori H, et al. Galectin-9 ameliorates clinical severity of MRL/lpr lupus-prone mice by inducing plasma cell apoptosis independently of Tim-3. PLoS One 2013;8:e60807.
25. Baba M, Wada J, Eguchi J, Hashimoto I, Okada T, Yasuhara A, et al. Galectin-9 inhibits glomerular hypertrophy in db/db diabetic mice via cell-cycle-dependent mechanisms. J Am Soc Nephrol 2005;16:3222–34.
26. Oomizu S, Arikawa T, Niki T, Kadowaki T, Ueno M, Nishi N, et al. Galectin-9 suppresses Th17 cell development in an IL-2-dependent but Tim-3-independent manner. Clin Immunol 2012;143:51–8.
27. Satoh M, Reeves WH. Induction of lupus-associated autoantibodies in BALB/c mice by intraperitoneal injection of pristane. J Exp Med 1994;180:2341–6.
28. Satoh M, Kumar A, Kanwar YS, Reeves WH. Anti-nuclear antibody production and immune-complex glomerulonephritis in BALB/c mice treated with pristane. Proc Natl Acad Sci U S A 1995;92:10934–8.
29. Reeves WH, Lee PY, Weinstein JS, Satoh M, Lu L. Induction of autoimmunity by pristane and other naturally occurring hydrocarbons. Trends Immunol 2009;30:455–64.
30. Potter M, Wax JS. Genetics of susceptibility to pristane-induced plasmacytomas in BALB/cAn: reduced susceptibility in BALB/cJ with a brief description of pristane-induced arthritis. J Immunol 1981;127:1591–5.
31. Watanabe-Fukunaga R, Brannan CI, Copeland NG, Jenkins NA, Nagata S. Lymphoproliferation disorder in mice explained by defects in Fas antigen that mediates apoptosis. Nature 1992; 356:314–7.
32. Adachi M, Suematsu S, Suda T, Watanabe D, Fukuyama H, Ogasawara J, et al. Enhanced and accelerated lymphoproliferation in Fas-null mice. Proc Natl Acad Sci U S A 1996;93:2131–6.
33. Seki M, Sakata KM, Oomizu S, Arikawa T, Sakata A, Ueno M, et al. Beneficial effect of galectin 9 on rheumatoid arthritis by induction of apoptosis of synovial fibroblasts. Arthritis Rheum 2007;56:3968–76.
34. Tsuboi Y, Abe H, Nakagawa R, Oomizu S, Watanabe K, Nishi N, et al. Galectin-9 protects mice from the Shwartzman reaction by attracting prostaglandin E2-producing polymorphonuclear leukocytes. Clin Immunol 2007;124:221–33.
35. Atkinson SM, Usher PA, Kvist PH, Markholst H, Haase C, Nansen A. Establishment and characterization of a sustained delayed-type hypersensitivity model with arthritic manifestations in C57BL/6J mice. Arthritis Res Ther 2012;14:R134.
36. Raatz Y, Ibrahim S, Feldmann M, Paleolog EM. Gene expression profiling and functional analysis of angiogenic markers in murine collagen-induced arthritis. Arthritis Res Ther 2012;14: R169.
37. Mannoor K, Matejuk A, Xu Y, Beardall M, Chen C. Expression of natural autoantibodies in MRL-lpr mice protects from lupus nephritis and improves survival. J Immunol 2012;188: 3628–38.
38. Ji H, Pettit A, Ohmura K, Ortiz-Lopez A, Duchatelle V, Degott C, et al. Critical roles for interleukin 1 and tumor necrosis factor α in antibody-induced arthritis. J Exp Med 2002;196:77–85.
39. Simon J, Surber R, Kleinstauber G, Petrow PK, Henzgen S, Kinne RW, et al. Systemic macrophage activation in locally-induced experimental arthritis. J Autoimmun 2001;17:127–36.
40. Carlucci F, Ishaque A, Ling GS, Szajna M, Sandison A, Donatien P, et al. C1q modulates the response to TLR7 stimulation by pristane-primed macrophages: implications for pristane-induced lupus. J Immunol 2016;196:1488–94.
41. Satoh M, Richards HB, Shaheen VM, Yoshida H, Shaw M, Naim JO, et al. Widespread susceptibility among inbred mouse strains to the induction of lupus autoantibodies by pristane. Clin Exp Immunol 2000;121:399–405.
42. Hamilton KJ, Satoh M, Swartz J, Richards HB, Reeves WH. Influence of microbial stimulation on hypergammaglobulinemia and autoantibody production in pristane-induced lupus. Clin Immunol Immunopathol 1998;86:271–9.
43. Shaheen VM, Satoh M, Richards HB, Yoshida H, Shaw M, Jennette JC, et al. Immunopathogenesis of environmentally induced lupus in mice. Environ Health Perspect 1999;107 Suppl 5:723–7.
44. Nacionales DC, Kelly KM, Lee PY, Zhuang H, Li Y, Weinstein JS, et al. Type I interferon production by tertiary lymphoid tissue developing in response to 2,6,10,14-tetramethyl-pentadecane (pristane). Am J Pathol 2006;168:1227–40.
45. Lee PY, Weinstein JS, Nacionales DC, Scumpia PO, Li Y, Butfiloski E, et al. A novel type I IFN-producing cell subset in murine lupus. J Immunol 2008;180:5101–8.
46. Lee PY, Kumagai Y, Li Y, Takeuchi O, Yoshida H, Weinstein J, et al. TLR7-dependent and FcγR-independent production of type I interferon in experimental mouse lupus. J Exp Med 2008; 205:2995–3006.
47. Arikawa T, Watanabe K, Seki M, Matsukawa A, Oomizu S, Sakata KM, et al. Galectin-9 ameliorates immune complex-induced arthritis by regulating FcγR expression on macrophages. Clin Immunol 2009;133:382–92.
48. Crispin JC, Oukka M, Bayliss G, Cohen RA, Van Beek CA, Stillman IE, et al. Expanded double negative T cells in patients

with systemic lupus erythematosus produce IL-17 and infiltrate the kidneys. J Immunol 2008;181:8761–6.
49. Kanzaki M, Wada J, Sugiyama K, Nakatsuka A, Teshigawara S, Murakami K, et al. Galectin-9 and T cell immunoglobulin mucin-3 pathway is a therapeutic target for type 1 diabetes. Endocrinology 2012;153:612–20.
50. Steelman AJ, Li J. Astrocyte galectin-9 potentiates microglial TNF secretion. J Neuroinflammation 2014;11:144.
51. Kanzler H, Barrat FJ, Hessel EM, Coffman RL. Therapeutic targeting of innate immunity with Toll-like receptor agonists and antagonists. Nat Med 2007;13:552–9.
52. Han J, Ulevitch RJ. Limiting inflammatory responses during activation of innate immunity. Nat Immunol 2005;6:1198–205.
53. Hagberg N, Ronnblom L. Systemic lupus erythematosus: a disease with a dysregulated type I interferon system. Scand J Immunol 2015;82:199–207.
54. Han S, Zhuang H, Xu Y, Lee P, Li Y, Wilson JC, et al. Maintenance of autoantibody production in pristane-induced murine lupus. Arthritis Res Ther 2015;17:384.
55. Heusschen R, Schulkens IA, van Beijnum J, Griffioen AW, Thijssen VL. Endothelial LGALS9 splice variant expression in endothelial cell biology and angiogenesis. Biochim Biophys Acta 2014;1842:284–92.
56. Ager A, May MJ. Understanding high endothelial venules: lessons for cancer immunology. Oncoimmunology 2015;4:e1008791.
57. Kageshita T, Kashio Y, Yamauchi A, Seki M, Abedin MJ, Nishi N, et al. Possible role of galectin-9 in cell aggregation and apoptosis of human melanoma cell lines and its clinical significance. Int J Cancer 2002;99:809–16.
58. Merani S, Chen W, Elahi S. The bitter side of sweet: the role of Galectin-9 in immunopathogenesis of viral infections. Rev Med Virol 2015;25:175–86.

Supplementary Figure 1

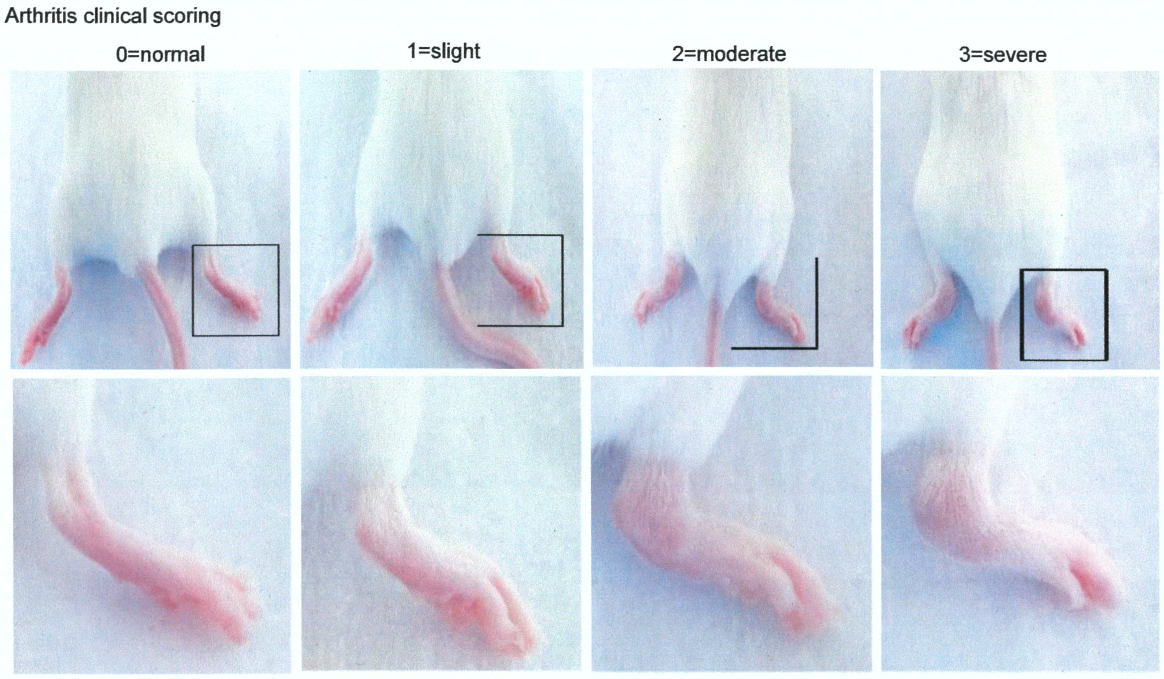

Supplementary Figure 2

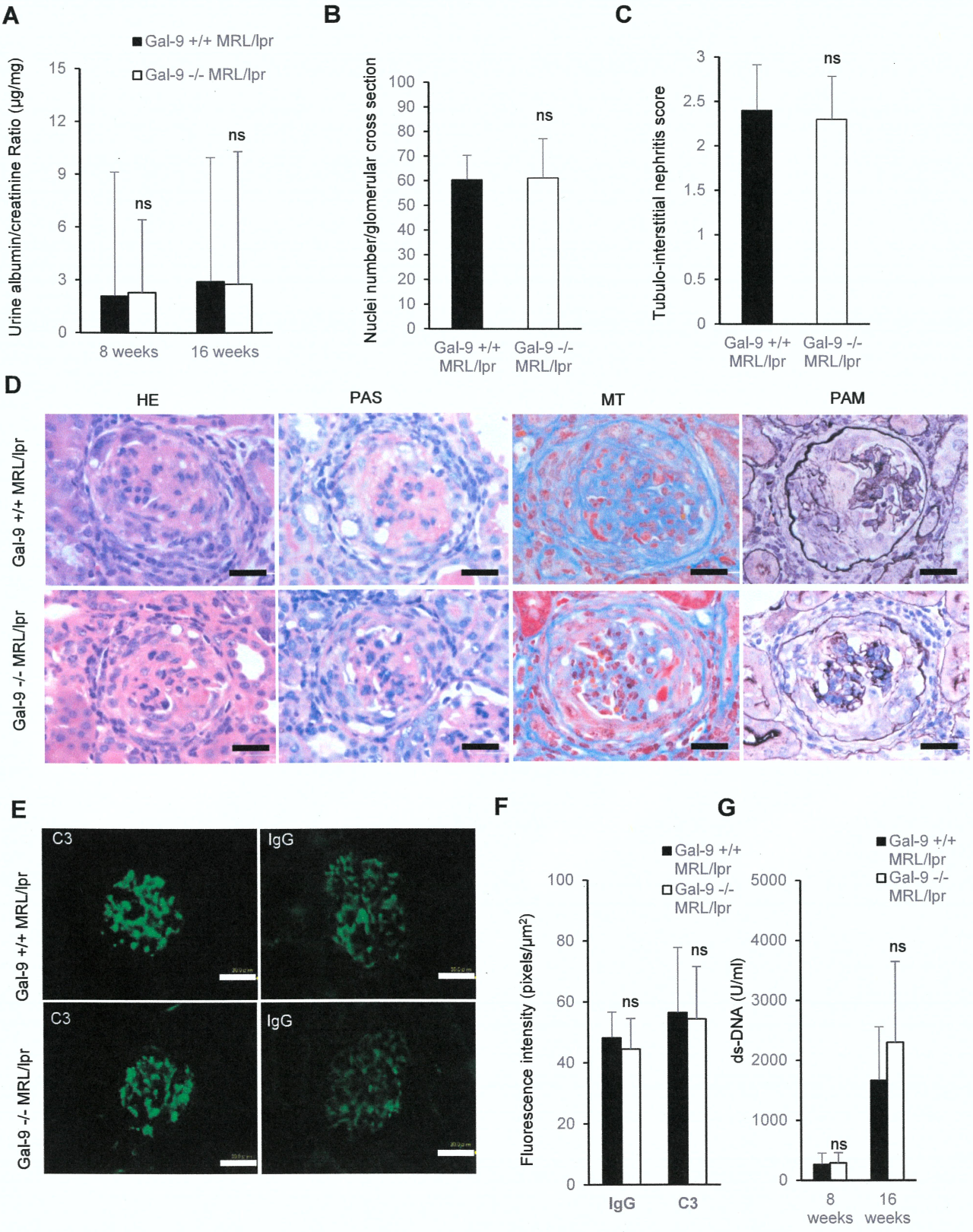

Supplementary Figure 3

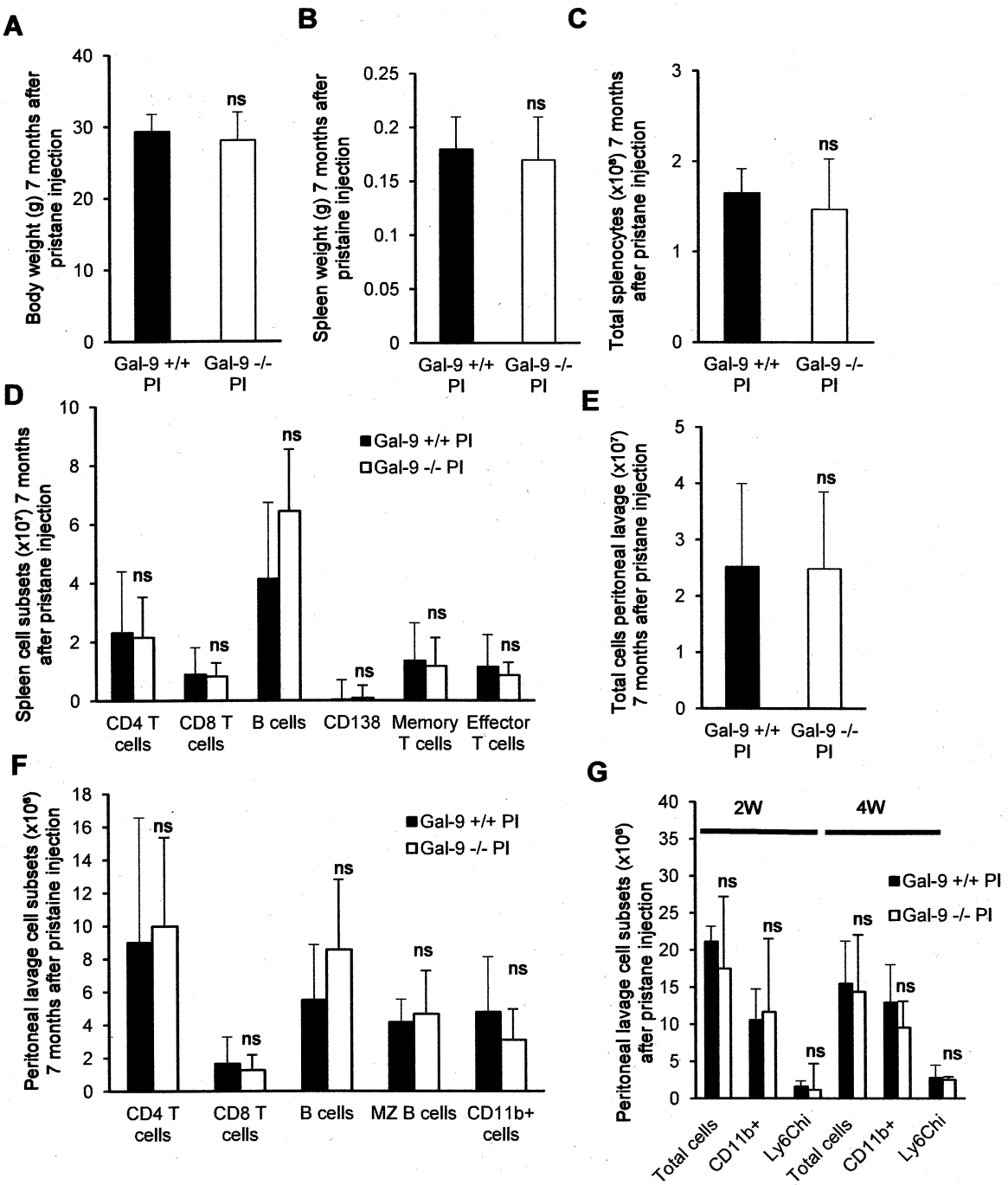

Supplementary Figure 4

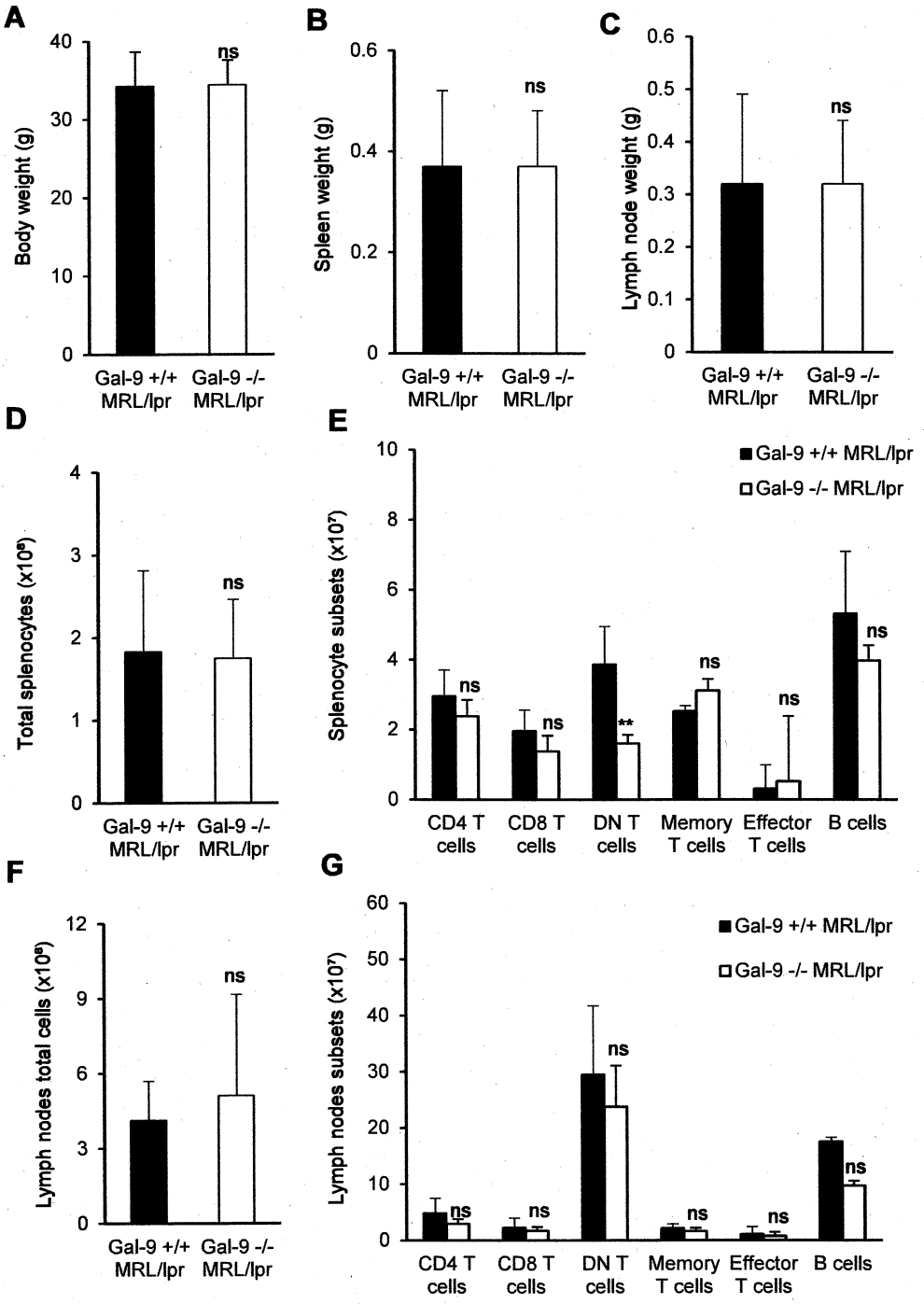

Supplementary Figure 5

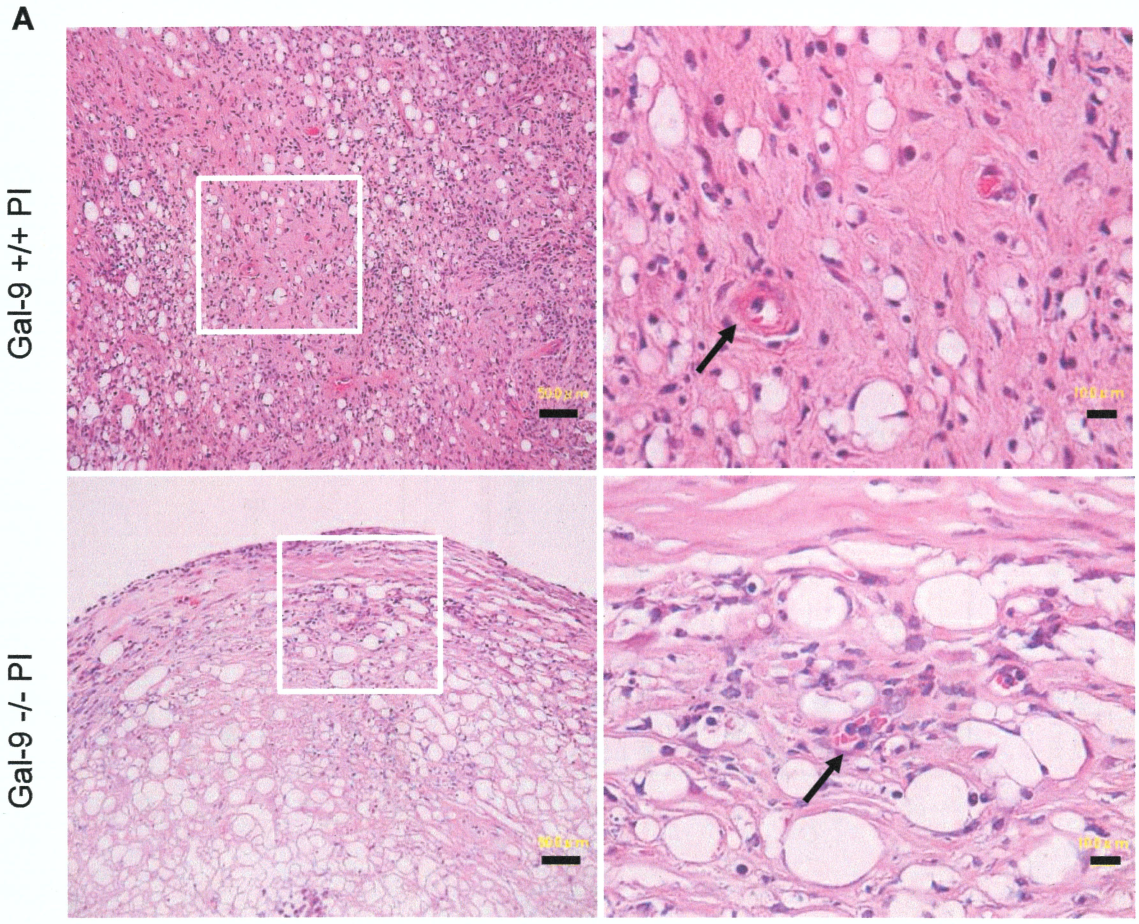

B

Figure 5D original figure

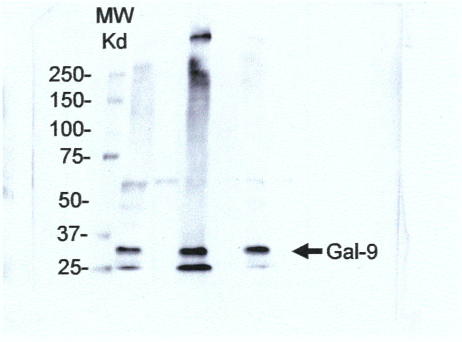

C

Figure 5D original figure

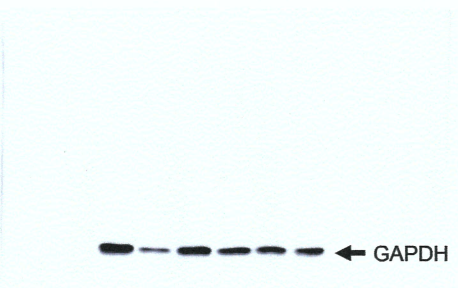

Supplementary Figure 6

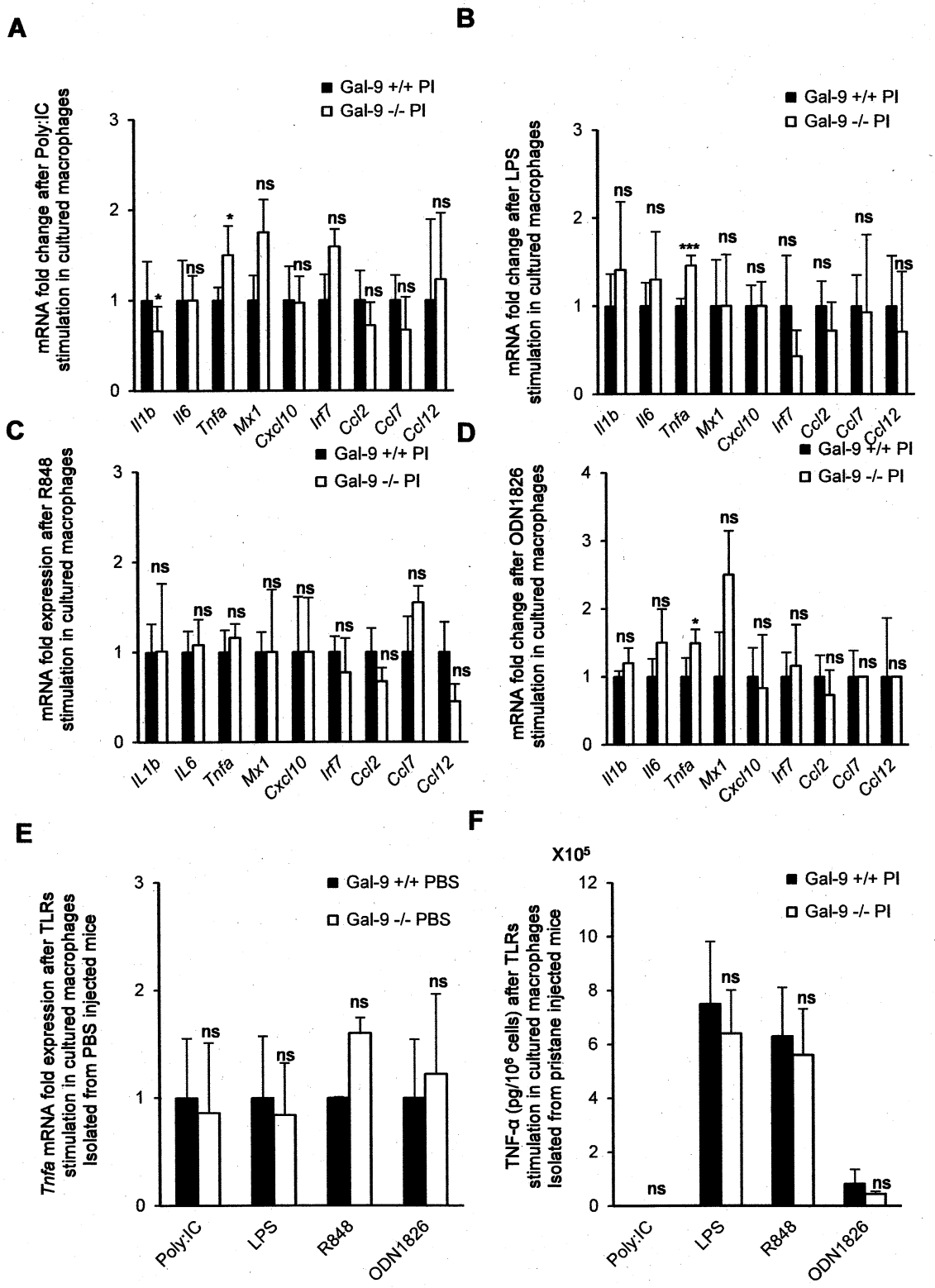

Supplementary Figure 1 Arthritis clinical scoring system in pristane injected BALB/c (PI) mice.

Representative pictures of back paws in normal and PI mice. In upper panels, the rectangle area is enlarged in the lower panels.

Supplementary Figure 2 Lupus nephritis in Gal-9 +/+ and Gal-9 -/- MRL/lpr mice.

A. Urinary albumin excretion in Gal-9 +/+ and Gal-9 -/- MRL/lpr mice (n=15). Mann-Whitney *U* test. **B.** Number of nuclei in glomeruli of Gal-9 +/+ and Gal-9 -/- MRL/lpr mice (n=15). Student's *t*-test. **C.** Tubulo-interstitial nephritis score in Gal-9 +/+ (n=15) and Gal-9 -/- (n=15) MRL/lpr mice. Student's *t*-test. **D.** Representative glomeruli with HE, PAS, MT and PAM in Gal-9 +/+ and Gal-9 -/- MRL/lpr mice. Aggressive nephritis with mesangial expansion, sclerosis, leucocyte infiltration and tubular damage in Gal-9 -/- MRL/lpr mice (scale bar 30 μm). **E.** Glomerular IgG and C3 deposition in MRL/lpr mice model. There is no difference in glomerular IgG and C3 deposition in Gal-9 +/+ and Gal-9 -/- MRL/lpr mice. Images are representative of 5 mice in each group (scale bar 30 μm). **F.** Computer-assisted quantification of immunofluorescence intensity of IgG deposits. There is no difference in Gal-9 +/+ and Gal-9 -/- MRL/lpr mice. Student's *t*-test. **G.** Levels of ds-DNA antibodies at 8 and 16 weeks in Gal-9 +/+ (n=6) and Gal-9 -/- MRL/lpr mice (n=6). *Lgals9* deficiency did not alter the levels of ds-DNA antibodies. Student's *t*-test. Data are presented as mean ± SD. $*p < 0.05$, $**p < 0.01$, $***p < 0.001$.

Supplementary Figure 3 Lymphocyte subsets in splenocytes and peritoneal lavage cells in Gal-9 +/+ and Gal-9 -/- PI mice.

Body weight **A** and spleen weight **B** 7 months after PI (n=11 in each group). **C**. Splenocytes counts 7 months after pristane injection. Cell numbers were determined using a hemocytometer (n=5 per group). **D.** Various lymphocyte subsets of splenocytes 7 months after PI. $CD3^+CD4^+$ (CD4 T cells), $CD3^+CD8^+$ (CD8 T cells), $CD19^+$ (B cells), $CD19^-$ $CD138^+$ (Plasma cells), $CD4^+CD44^+CD62L^+$ (Memory T cells), $CD4^+CD44^+CD62L^-$ (Effector T cells). Absolute number of cellular subsets isolated from whole spleen are indicated in Gal-9 +/+ (n=5) and Gal-9 -/- PI (n=5) mice. **E.** Total peritoneal cell count 7 months after PI. Total cell counts were determined by hemocytometer (n=5 per group). **F and G.** Influx of inflammatory leucocytes into the peritoneal cavity 7 months and 15 days following PI. The peritoneal cells were harvested, stained and analyzed for different cell subsets by flow cytometry 7 months (**F**; n=5 per group), 15 days (**G**; n=4 per group), and 4 weeks (**G**; n=3 per group) after PI. $CD19^+B220^+$ [marginal zone (MZ) B cells], CD11b+Ly6C+Ly6G- ($Ly6C^{High}$). Data are presented as mean ± SD. $*p < 0.05$, $**p < 0.01$, $***p < 0.001$. Student's *t*-test.

Supplementary Figure 4 Lymphocyte subsets in spleen and lymph nodes in Gal-9 +/+ and Gal-9 -/- MRL/lpr mice.

Body weight (**A**) and spleen weight (**B**) and lymph nodes weight (**C**) at 16 weeks in MRL/lpr Gal-9 +/+ (n=15) and Gal-9 -/- (n=15) MRL/lpr. **D**. Splenocytes cell counts at 16 weeks in Gal-9 +/+ (n=6) and Gal-9 -/- (n=6) MRL/lpr. **E.** Various cellular subsets in spleen of MRL/lpr. The absolute number of cell subsets in spleen of 16 weeks Gal-9 +/+ (n=4) and Gal-9 -/- (n=4) MRL/lpr. $CD3^{+}CD4^{-}CD8^{-}$ [Double negative (DN) T cells]. **F.** Lymph nodes cell count in Gal-9 +/+ (n=6) and Gal-9 -/- (n=6) MRL/lpr. Total cell counts were determined using a hemocytometer. **G.** Absolute cell number of various cellular subsets in lymph nodes of MRL/lpr mice. Lymph nodes cells were isolated, stained and analyzed for different cell subsets by flow cytometry (n=4 per group). Data are presented as mean ± SD. $*p < 0.05$, $**p < 0.01$, $***p < 0.001$. Student's *t*-test.

Supplementary Figure 5 *Tnfa* transcription and secretion overtime and ISG expression in peritoneal macrophages of PI mice

A. Representative histopathological sections stained with HE in ectopic lymphoid tissue 7 months after pristane injection from Gal-9 +/+ PI (n=10) and Gal-9 -/- PI mice (n=12). High endothelial venules (HEVs) are shown by arrows. (Scale bars; left panel 50 μm and right panel 10 μm) **B** and **C**. Western blot analysis of Gal-9 in lipogranuloma, spleen and lymph nodes of Gal-9 -/- PI and Gal-9 +/+ PI mice. Data are presented as mean ± SD. $*p < 0.05$, $**p < 0.01$, $***p < 0.001$. Student's *t*-test.

Supplementary Figure 6 mRNA expression of cytokines in peritoneal macrophage recruited either with pristane or PBS and stimulated with different TLRs ligands.

A. *Il1*, *Il6*, *Tnfa,* ISG and chemokines expression at 24 hours after stimulation with TLR3 ligand, Poly: IC. **B.** *Il1*, *Il6*, *Tnfa,* ISG and chemokines expression at 24 hours after stimulation with TLR4 ligand, LPS. **C.** *Il1*, *Il6*, *Tnfa,* ISG and chemokines expression at 24 hours after stimulation with TLR7 ligand, R848. **D.** *Il1*, *Il6*, *Tnfa,* ISG and chemokines expression at 24 hours after stimulation with TLR9 ligand, ODN 1826.Images are representative of 5 mice per group (n=5). **E.** *Tnfa* expression at 24 hours after stimulation with TLRs ligands in cultured peritoneal macrophages isolated at 24 hours after PBS injection (n=3). Expression levels were assessed by RT-PCR. **F.** TNFα production in the culture supernatant at 24 hours after stimulation with TLRs ligands in cultured peritoneal macrophages isolated at 24 hours after pristane injection isolated from Gal-9 -/- mice and Gal-9 +/+ mice. Protein levels were assessed using ELISA (n=5 per group). Data are presented as mean ± SD. $*p < 0.05$, $**p < 0.01$, $***p < 0.001$. Student's *t*-test.